DOI:
10.1109/TFUZZ.2019.2907503

Document Version
Peer reviewed version

Sampled-Data Output-Feedback Tracking Control for Interval Type-2 Polynomial Fuzzy Systems

Bo Xiao, *Member, IEEE*, Hak-Keung Lam, *Senior Member, IEEE*, Yan Yu and Yuandi Li

***Abstract*—In this paper, the stability and performance of the interval type-2 (IT2) polynomial fuzzy-model-based (PFMB) tracking control system, formed by an IT2 polynomial fuzzy model and an IT2 polynomial fuzzy controller, based on the output feedback and sampled-data structure are investigated. IT2 fuzzy sets are employed to capture the uncertainties of the nonlinear plant. Furthermore, considering the digital implementation of control strategy and only the system outputs are available, the IT2 polynomial fuzzy controller is of discrete time and output-feedback type. Both membership-function-independent and membership-function-dependent stability analysis, with the consideration of H_∞ performance index, are conducted to develop stability conditions in terms of sum-of-square (SOS) based on Lyapunov stability theory. The information of membership functions, system states and sampling process are included in the stability analysis for the relaxation of stability conditions. Simulation examples are presented to verify the effectiveness of the proposed tracking control approach.**

***Index Terms*—Interval Type-2 (IT2) fuzzy logic, Polynomial fuzzy-model-based (PFMB) control systems, Stability analysis, Sum of squares (SOS), Sampled-data output, Tracking control.**

I. Introduction

FUZZY-model-based (FMB) control strategies have been successfully applied to deal with the stabilization, regulation and tracking control problems for nonlinear systems. In those control strategies, the Takagi-Sugeno (T-S) fuzzy model [1] plays an important role in the FMB control design thanks to its favorable model structure in support of system analysis and control design. Based on Lyapunov stability theory, stability conditions [1] in terms of linear matrix inequalities (LMIs) have been developed to determine the system stability and synthesize the controller. There are fruitful works based on T-S FMB control systems in terms of both stability analysis and applications [1]–[5]. Also, it is reported that when the affine terms are included into T-S models, the nonlinear approximation ability of T-S fuzzy systems can be further improved [6], [7].

Tracking control problem is always met in many control applications. In the tracking control design, the controller does not only stabilize the control system but also drives the states of the nonlinear plant to follow a reference signal or the system states of a stable reference model [8]. Therefore, the tracking control problem is generally considered more challenging than the stabilization problem. When only the system output is available, output-feedback control is one of the methods to be considered. Furthermore, employing a digital computer or microcontroller to realize the controller is possible to reduce the implementation time and costs. With all these considerations, sampled-data output-feedback (SDOF) fuzzy control strategy would be a candidate control method to deal with the tracking control problem for nonlinear plants.

The work in [8] introduced a fuzzy tracking control technique where H_∞ performance is considered to attenuate the tracking error to a prescribed level. The fuzzy control concept was then combined with output-feedback control method, resulting in output-feedback fuzzy tracking control strategy [9]–[12], which requires only the system output instead of full state for feedback compensation. Also, with the consideration of digital control application, SDOF fuzzy tracking control strategy was introduced in [13] and extended to polynomial fuzzy-model-based (PFMB) control systems [14], [15]. Polynomial fuzzy models can be regarded as the generalization of T-S fuzzy models. When the order of the polynomial terms is reduced to 0, the polynomial fuzzy model will become a T-S one. It is also worth mentioning that polynomial fuzzy models have better global approximation ability, which helps reduce the number of fuzzy rules when compared with the T-S counterpart [16].

The most popular type of membership functions used in the FMB/PFMB control systems is of type-1 fuzzy set which is applied to tackle the nonlinearities in control systems but it lacks the ability to deal with uncertainties directly [17], [18]. To include the uncertainties directly into the membership functions, the concept of footprint of uncertainty (FOU) along with the type-2 fuzzy sets [17] was introduced. To alleviate the computational burden raised by type reduction of type-2 fuzzy sets, the interval type-2 (IT2) fuzzy sets [17] are introduced. A novel IT2 fuzzy model and its construction were proposed for the first time in [18] under the FMB control framework followed by an innovative membership-function-dependent (MFD) stability analysis techniques [19]. Other follow-up works can be found in [20], [21]. Recent type-2 fuzzy sets related works expanded with other topics such as random delays, limited communication capacity and time-delay partition can also be found in [22]–[24]. In addition, recent type-2 fuzzy sets related works such as type-reduction and control applications of type-2 fuzzy sets to aerospace, airplane flight control, mobile robots and UAVs can be found in [25]–[33].

A controller can be implemented with a microcontroller or a digital computer at low costs. However, the closed-loop control system becomes a sampled-data control system. Due

The work described in this paper was partly supported by King's College London and Chinese Scholarship Council.

Bo Xiao, Hak-Keung Lam, Yan Yu and Yuandi Li are with the Department of Informatics, King's College London, Bush House, Strand campus, 30 Aldwych, London, WC2B 4BG, U.K. e-mail: {b.xiao@imperial.ac.uk, hak-keung.lam, yan.yu, yuandi.li}@kcl.ac.uk.

to the zero-order-hold (ZOH), the sampled states/outputs are of staircase signal. The discrete singal causes discontinuity in the control input, which complicates the system dynamics for system analysis and control design. To deal with the hybrid system dynamics in the context of FMB/PFMB control systems, the input-delay approach [20], [34], equivalent jump system [35], discretization approach [36], digital redesign [37], [38] and the exact discrete-time design approach [39] can be used for stability analysis and control design.

In this paper, we consider both the stability and performance of the SDOF PFMB tracking control problem, which has received less attention in the field. To start with the investigation, an IT2 polynomial fuzzy model is employed to represent the dynamics of the nonlinear plant subject to uncertainties captured by IT2 fuzzy sets. Sampled-data output-feedback polynomial fuzzy controller is then employed to realize the tracking control so that the system states are driven to follow those of a reference model. where the tracking error is governed by an H_∞ performance index. Due to the existence of uncertainties, the premise membership grades become uncertain which prevents the parallel distributed compensation (PDC)-based stability analysis [1] to be applied for the reason that it requires the premise membership functions of the fuzzy model and fuzzy controller to be exactly the same. To address the problem, we consider that the premise membership functions and/or number of rules can be different. The Lyapunov-Krasovskii functional is adopted to facilitate the stability analysis with the support of the information of lower and upper membership functions characterizing the FOU. Due to ZOH, the membership functions of the fuzzy controller can only be evaluated at the sampling instants, which makes it difficult to extract useful information from membership functions during the sampling period for the stability analysis. To circumvent this difficulty, the lower and upper membership functions, which captures the uncertainties within the FOU are considered. Both sets of sum-of-square (SOS)-based membership-function-independent (MFI) and MFD stability conditions are obtained to determine the system stability and synthesize the controller. For the stability conditions, the MFI stability conditions do not take any information of membership functions into account while the MFD ones which contain the information of membership functions. Consequently, the MFD stability conditions are more relaxed but generally more computational demanding compared with the MFI ones [40]. To the authors' best knowledge, this is the first attempt to adopt IT2 polynomial fuzzy model to deal with sampled-data tracking control problems.

The main contributions of this paper are: 1) The sampled-data output-feedback case is investigated for the purpose of digital application. 2) The characteristics of the IT2 membership functions are utilized to incorporate uncertainties in the nonlinear plant to the FOU. 3) The unknown difference between the unmeasurable real output and the measurable sampled output is embedded in the IT2 membership functions.

The rest of the paper is organized as follows: In Section II, the preliminaries of the tracking control system will be introduced. In Section III, the stability analysis will be discussed in details. In Section IV, two simulation examples are presented to verify effectiveness of the proposed control strategy. In Section V, a conclusion is drawn.

II. Preliminaries

Polynomial fuzzy models, the IT2 polynomial fuzzy model, reference model and IT2 SDOF polynomial fuzzy controller are introduced in this section.

A. IT2 Polynomial Fuzzy Model

An IT2 polynomial fuzzy model with p rules of the following format is employed to describe the dynamics of nonlinear plant [18], [19], [21].

Rule i : IF $f_1(\mathbf{x}(t))$ is $\tilde{M}_1^i$ AND $\cdots$ AND $f_\Psi(\mathbf{x}(t))$ is $\tilde{M}_\Psi^i$

$$\text{THEN } \dot{\mathbf{x}}(t) = \mathbf{A}_i(\mathbf{x}(t))\hat{\mathbf{x}}(\mathbf{x}(t)) + \mathbf{B}_i(\mathbf{x}(t))\mathbf{u}(t), \quad (1)$$

$$\mathbf{y}(t) = \mathbf{C}\hat{\mathbf{x}}(\mathbf{x}(t)) \quad (2)$$

where $\tilde{M}_\alpha^i$ is a fuzzy term of rule i corresponding to the known function $f_\alpha(\mathbf{x}(t))$, $\alpha = 1, 2, \ldots, \Psi$ and $i = 1, 2, \ldots, p$; Ψ is a positive integer; $\mathbf{A}_i(\mathbf{x}(t)) \in \Re^{n\times N}$ and $\mathbf{B}_i(\mathbf{x}(t)) \in \Re^{n\times m}$ are the known polynomial system and input matrices; $\mathbf{x}(t) \in \Re^n$ is the state vector, $\hat{\mathbf{x}}(\mathbf{x}(t)) \in \Re^N$ is a vector of monomials in $\mathbf{x}(t)$, and $\mathbf{u}(t) \in \Re^m$ is the control input vector, $\mathbf{C} \in \Re^{q\times N}$ is the constant output matrix, $\mathbf{y}(t) \in \Re^q$ is the system output vector. It is assumed that $\hat{\mathbf{x}}(t) = \mathbf{0}$ when $\mathbf{x}(t) = \mathbf{0}$. Since dimensions of $\mathbf{B}_i(\mathbf{x}(t))$ and $\mathbf{C}$ are defined to allow m inputs and q outputs of the control system, the IT2 polynomial fuzzy system can be also treated as the Multi-input multi-output (MIMO) system. The i-th rule's firing strength is within the following interval sets:

$$\tilde{w}_i(\mathbf{x}(t)) \in [w_i^L(\mathbf{x}(t)), w_i^U(\mathbf{x}(t))], \quad i = 1, 2, \ldots, p \quad (3)$$

where $w_i^L(\mathbf{x}(t)) = \prod_{\alpha=1}^{\Psi} \underline{\mu}_{\tilde{M}_\alpha^i}(f_\alpha(\mathbf{x}(t)))$ and $w_i^U(\mathbf{x}(t)) = \prod_{\alpha=1}^{\Psi} \overline{\mu}_{\tilde{M}_\alpha^i}(f_\alpha(\mathbf{x}(t)))$ in which $0 \le \overline{\mu}_{\tilde{M}_\alpha^i}(f_\alpha(\mathbf{x}(t))) \le 1$ and $0 \le \underline{\mu}_{\tilde{M}_\alpha^i}(f_\alpha(\mathbf{x}(t))) \le 1$ denote the upper and lower grades of membership governed by their upper and lower membership functions, respectively. By the definition of IT2 membership functions, the property $0 \le \underline{\mu}_{\tilde{M}_\alpha^i}(f_\alpha(\mathbf{x}(t))) \le \overline{\mu}_{\tilde{M}_\alpha^i}(f_\alpha(\mathbf{x}(t))) \le 1$ holds, which further leads to $0 \le w_i^L(\mathbf{x}(t)) \le w_i^U(\mathbf{x}(t)) \le 1$ for all i. $\tilde{w}_i(\mathbf{x}(t))$ is defined as follows: $\tilde{w}_i(\mathbf{x}(t)) = \underline{\lambda}_i(\mathbf{x}(t))w_i^L(\mathbf{x}(t)) + \overline{\lambda}_i(\mathbf{x}(t))w_i^U(\mathbf{x}(t))$, $0 \le \underline{\lambda}_i(\mathbf{x}(t)) \le 1$, $0 \le \overline{\lambda}_i(\mathbf{x}(t)) \le 1$, $\underline{\lambda}_i(\mathbf{x}(t)) + \overline{\lambda}_i(\mathbf{x}(t)) = 1, \forall\, i$, where $\underline{\lambda}_i(\mathbf{x}(t))$ and $\overline{\lambda}_i(\mathbf{x}(t))$ are nonlinear functions, which are not necessary to be known but exist.

The IT2 polynomial fuzzy model is described by

$$\dot{\mathbf{x}}(t) = \sum_{i=1}^{p} \tilde{w}_i(\mathbf{x}(t))(\mathbf{A}_i(\mathbf{x}(t))\hat{\mathbf{x}}(\mathbf{x}(t)) + \mathbf{B}_i(\mathbf{x}(t))\mathbf{u}(t)) \quad (4)$$

where $\sum_{i=1}^{p} \tilde{w}_i(\mathbf{x}(t)) = 1$, $\tilde{w}_i(\mathbf{x}(t)) \ge 0\ \forall\, i$ and the output of the polynomial fuzzy model is described by

$$\mathbf{y}(t) = \mathbf{C}\hat{\mathbf{x}}(\mathbf{x}(t)). \quad (5)$$

B. Reference Model

A stable reference model is defined as follows:

$$\dot{\mathbf{x}}_\mathbf{r}(t) = \mathbf{A}_\mathbf{r}\hat{\mathbf{x}}_\mathbf{r}(\mathbf{x}_\mathbf{r}(t)) + \mathbf{B}_\mathbf{r}\mathbf{r}(t), \mathbf{y}_\mathbf{r}(t) = \mathbf{C}\hat{\mathbf{x}}_\mathbf{r}(\mathbf{x}_\mathbf{r}(t)) \quad (6)$$

where $\mathbf{x_r}(t) \in \Re^n$ is the reference system state vector, which needs to be followed by the IT2 polynomial fuzzy model (4), $\hat{\mathbf{x}}_\mathbf{r}(\mathbf{x_r}(t)) \in \Re^N$ is a vector of monomials in $\mathbf{x_r}(t)$ as the entries, $\mathbf{A_r} \in \Re^{n\times N}$ and $\mathbf{B_r} \in \Re^{n\times m}$ are the constant system and input matrices, respectively, $\mathbf{r}(t) \in \Re^m$ is the reference input vector, $\mathbf{y_r}(t) \in \Re^q$ is the reference output state vector. It is worth mentioning that the reference model describes the dynamics of a stable system. The IT2 SDOF polynomial fuzzy controller is designed to drive $\mathbf{x}(t)$ to follow $\mathbf{x_r}(t)$.

C. IT2 SDOF Polynomial Fuzzy Controller

Define the state error (or tracking error of states) as follows:

$$\hat{\mathbf{e}}(t) = \hat{\mathbf{x}}(\mathbf{x}(t)) - \hat{\mathbf{x}}_\mathbf{r}(\mathbf{x_r}(t)). \tag{7}$$

From (4), (6) and (7), the output error is defined as follows:

$$\mathbf{e_y}(t) = \mathbf{y}(t) - \mathbf{y_r}(t) = \mathbf{C}\hat{\mathbf{e}}(t). \tag{8}$$

An IT2 SDOF polynomial fuzzy controller with c rules of the following format is employed to drive the states of the nonlinear plant represented by the IT2 polynomial fuzzy model (4) to follow those of the reference model (6) where the tracking error $\hat{\mathbf{e}}(t)$ is characterized by H_∞ performance.

Rule j : IF $g_1(\mathbf{y}(t_\gamma))$ is $\tilde{N}_1^j$ AND $\cdots$ AND $g_\Omega(\mathbf{y}(t_\gamma))$ is $\tilde{N}_\Omega^j$
THEN $\mathbf{u}(t) = \mathbf{F}_j(\mathbf{h}(t_\gamma))\mathbf{e_y}(t_\gamma) + \mathbf{G}_j(\mathbf{h}(t_\gamma))\mathbf{y_r}(t_\gamma)$ (9)

where $\tilde{N}_\beta^j$ is an IT2 fuzzy term of rule j corresponding to function $g_\beta(\mathbf{y}(t))$, where $\beta = 1, 2, \ldots, \Omega$ and $j = 1, 2, \ldots, c$; Ω is a positive integer. $t_\gamma = t - \tau(t)$, for $t_\gamma < t \le t_{\gamma+1}$, $0 \le \tau(t) \le h_s$, h_s is the sampling period and t_γ is the time at the γ-th sampling instant. Define $\mathbf{h}(t_\gamma) = [\mathbf{y}(t_\gamma) \quad \mathbf{y_r}(t_\gamma)]$, and $\mathbf{F}_j(\mathbf{h}(t_\gamma)) \in \Re^{m\times q}$ and $\mathbf{G}_j(\mathbf{h}(t_\gamma)) \in \Re^{m\times q}$, j = 1, 2, …, c, as the polynomial feedback gains to be determined. The j-th rule's firing strength is within the following interval sets:

$$\tilde{m}_j(\mathbf{y}(t_\gamma)) \in [m_j^L(\mathbf{y}(t_\gamma)), m_j^U(\mathbf{y}(t_\gamma))], \quad j = 1, 2, \ldots, c \tag{10}$$

where $m_j^L(\mathbf{y}(t_\gamma)) = \prod_{r=1}^{\Omega} \underline{\mu}_{\tilde{N}_\beta^j}(g_\beta(\mathbf{y}(t_\gamma)))$, $m_j^U(\mathbf{y}(t_\gamma)) = \prod_{r=1}^{\Omega} \overline{\mu}_{\tilde{N}_\beta^j}(g_\beta(\mathbf{y}(t_\gamma)))$ in which $0 \le \overline{\mu}_{\tilde{N}_\beta^j}(g_\beta(\mathbf{y}(t_\gamma))) \le 1$ and $0 \le \underline{\mu}_{\tilde{N}_\beta^i}(g_\beta(\mathbf{y}(t_\gamma))) \le 1$ denote the upper and lower grades of membership governed by the upper and lower membership functions, respectively. By the definition of IT2 membership functions, the property $0 \le \underline{\mu}_{\tilde{N}_\beta^j}(g_\beta(\mathbf{y}(t_\gamma))) \le \overline{\mu}_{\tilde{N}_\beta^j}(g_\beta(\mathbf{y}(t_\gamma))) \le 1$ holds and further leads to $0 \le m_j^L(\mathbf{y}(t_\gamma)) \le m_j^U(\mathbf{y}(t_\gamma)) \le 1$, which is valid for all j.

Inspired by [18], $\tilde{m}_j(\mathbf{y}(t_\gamma))$ is defined as follows:

$$0 \le \tilde{m}_j(\mathbf{y}(t_\gamma)) = \frac{\underline{\kappa}_j(\mathbf{y}(t_\gamma))m_j^L(\mathbf{y}(t_\gamma)) + \overline{\kappa}_j(\mathbf{y}(t_\gamma))m_j^U(\mathbf{y}(t_\gamma))}{\sum_{k=1}^{c}\left(\underline{\kappa}_k(\mathbf{y}(t_\gamma))m_k^L(\mathbf{y}(t_\gamma)) + \overline{\kappa}_k(\mathbf{y}(t_\gamma))m_k^U(\mathbf{y}(t_\gamma))\right)} \tag{11}$$

where $0 \le \underline{\kappa}_j(\mathbf{y}(t_\gamma)) \le 1$, $0 \le \overline{\kappa}_j(\mathbf{y}(t_\gamma)) \le 1$, $\underline{\kappa}_j(\mathbf{y}(t_\gamma)) + \overline{\kappa}_j(\mathbf{y}(t_\gamma)) = 1$, $\forall$ j; $\underline{\kappa}_j(\mathbf{y}(t_\gamma))$ and $\overline{\kappa}_j(\mathbf{y}(t_\gamma))$ are nonlinear functions to be determined. The IT2 SDOF polynomial fuzzy controller is described by the following:

$$\mathbf{u}(t) = \sum_{j=1}^{c} \tilde{m}_j(\mathbf{y}(t_\gamma))(\mathbf{F}_j(\mathbf{h}(t_\gamma))\mathbf{e_y}(t_\gamma) + \mathbf{G}_j(\mathbf{h}(t_\gamma))\mathbf{y_r}(t_\gamma)) \tag{12}$$

where $\sum_{i=1}^{c} \tilde{m}_j(\mathbf{y}(t_\gamma)) = 1$ and $\tilde{m}_j(\mathbf{y}(t_\gamma)) \ge 0 \;\forall\; j$.

III. Stability Analysis

The tracking control problem for the IT2 SDOF PFMB control system, formed by the IT2 polynomial fuzzy model (4), reference model (6) and the SDOF polynomial fuzzy controller (12) discussed in the previous section, is considered through stability analysis in this section. The tracking performance is characterized by an H_∞ performance index. Both sets of MFI and MFD stability conditions are obtained to determine the system stability and synthesize the feedback gains.

For brevity, in the following analysis, the time t associated with the variables is dropped for the situation without ambiguity, e.g., $\hat{\mathbf{e}}(t)$, $\mathbf{e_y}(t)$, $\mathbf{x}(t)$, $\hat{\mathbf{x}}_\mathbf{r}(\mathbf{x_r}(t))$ and $\hat{\mathbf{x}}(\mathbf{x}(t))$ are denoted as $\hat{\mathbf{e}}$, $\mathbf{e_y}$, $\mathbf{x}$, $\hat{\mathbf{x}}_\mathbf{r}(\mathbf{x_r})$ and $\hat{\mathbf{x}}(\mathbf{x})$, respectively. In matrices, "*" denotes the transposed element at the corresponding position.

A. Basic MFI Stability Conditions with H_∞ Performance

Combining (4) and (12), we get the closed-loop dynamic as

$$\dot{\mathbf{x}} = \sum_{i=1}^{p}\sum_{j=1}^{c} \tilde{w}_i(\mathbf{x})\tilde{m}_j(\mathbf{y}(t_\gamma))\big(\mathbf{A}_i(\mathbf{x})\hat{\mathbf{x}} + \mathbf{B}_i(\mathbf{x})(\mathbf{F}_j(\mathbf{h}(t_\gamma))\mathbf{e_y}(t_\gamma) + \mathbf{G}_j(\mathbf{h}(t_\gamma))\mathbf{y_r}(t_\gamma))\big), \tag{13}$$

in which $\mathbf{x} = [x_1, x_2, \ldots, x_n]^T$ and $\hat{\mathbf{x}}(\mathbf{x}) = [\hat{x}_1(\mathbf{x}), \hat{x}_2(\mathbf{x}), \ldots, \hat{x}_N(\mathbf{x})]$.

Let us consider the relationship between $\dot{\hat{\mathbf{x}}}$ and $\dot{\mathbf{x}}$, which can be linked together by $\mathbf{T}(\mathbf{x})$ as follows:

$$\dot{\hat{\mathbf{x}}} = \frac{\partial\hat{\mathbf{x}}}{\partial\mathbf{x}}\frac{d\mathbf{x}}{dt} = \mathbf{T}(\mathbf{x})\dot{\mathbf{x}}, \tag{14}$$

where $\mathbf{T}(\mathbf{x}) \in \Re^{N\times n}$ with its $\alpha\beta$-th element is defined as

$$T_{\alpha\beta}(\mathbf{x}) = \frac{\partial\hat{x}_\alpha(\mathbf{x})}{\partial x_\beta}, \alpha = 1, 2, \ldots, N; \beta = 1, 2, \ldots, n. \tag{15}$$

From (13) and (14), we have

$$\dot{\hat{\mathbf{x}}} = \sum_{i=1}^{p}\sum_{j=1}^{c} \tilde{w}_i(\mathbf{x})\tilde{m}_j(\mathbf{y}(t_\gamma))\big(\tilde{\mathbf{A}}_i(\mathbf{x})\hat{\mathbf{x}} + \tilde{\mathbf{B}}_i(\mathbf{x})(\mathbf{F}_j(\mathbf{h}(t_\gamma))\mathbf{e_y}(t_\gamma) + \mathbf{G}_j(\mathbf{h}(t_\gamma))\mathbf{y_r}(t_\gamma))\big) \tag{16}$$

where $\tilde{\mathbf{A}}_i(\mathbf{x}) = \mathbf{T}(\mathbf{x})\mathbf{A}_i(\mathbf{x})$, $\tilde{\mathbf{B}}_i(\mathbf{x}) = \mathbf{T}(\mathbf{x})\mathbf{B}_i(\mathbf{x})$.

Denote $\mathbf{x_r} = [x_{r_1}, x_{r_2}, \ldots, x_{r_n}]^T$ and $\hat{\mathbf{x}}_\mathbf{r}(\mathbf{x_r}) = [\hat{x}_{r_1}(\mathbf{x_r}), \hat{x}_{r_2}(\mathbf{x_r}), \ldots, \hat{x}_{r_N}(\mathbf{x_r})]^T$. From (6), we have the polynomial dynamic model for the reference model:

$$\dot{\hat{\mathbf{x}}}_\mathbf{r}(\mathbf{x_r}) = \mathbf{H}(\mathbf{x_r})\dot{\mathbf{x}}_\mathbf{r} = \tilde{\mathbf{A}}_\mathbf{r}(\mathbf{x_r})\hat{\mathbf{x}}(\mathbf{x_r}) + \tilde{\mathbf{B}}_\mathbf{r}(\mathbf{x_r})\mathbf{r} \tag{17}$$

where $\tilde{\mathbf{A}}_\mathbf{r}(\mathbf{x_r}) = \mathbf{H}(\mathbf{x_r})\mathbf{A_r}$, $\tilde{\mathbf{B}}_\mathbf{r}(\mathbf{x_r}) = \mathbf{H}(\mathbf{x_r})\mathbf{B_r}$ and $\mathbf{H}(\mathbf{x_r}) \in \Re^{N\times n}$ with its $\alpha\beta$-th element is defined as

$$H_{\alpha\beta}(\mathbf{x_r}) = \frac{\partial\hat{x}_{r_\alpha}(\mathbf{x})}{\partial x_{r_\beta}}, \alpha = 1, 2, \ldots, N; \beta = 1, 2, \ldots, n. \tag{18}$$

Also, from (7), combining the polynomial dynamic model in (17) with (16), $\dot{\hat{\mathbf{e}}}$ can be expressed as follows:

$$\begin{aligned}\dot{\hat{\mathbf{e}}} &= \sum_{i=1}^{p}\sum_{j=1}^{c}\tilde{w}_i(\mathbf{x})\tilde{m}_j(\mathbf{y}(t_\gamma))\big(\tilde{\mathbf{A}}_i(\mathbf{x})\hat{\mathbf{e}}\\&+\tilde{\mathbf{B}}_i(\mathbf{x})\mathbf{F}_j(\mathbf{h}(t_\gamma))\mathbf{C}\hat{\mathbf{e}}(t_\gamma)\big)\\&+\sum_{i=1}^{p}\sum_{j=1}^{c}\tilde{w}_i(\mathbf{x})\tilde{m}_j(\mathbf{y}(t_\gamma))\big((\tilde{\mathbf{A}}_i(\mathbf{x})-\tilde{\mathbf{A}}_{\mathbf{r}}(\mathbf{x_r}))\hat{\mathbf{x}}_{\mathbf{r}}(\mathbf{x_r})\\&+\tilde{\mathbf{B}}_i(\mathbf{x})\mathbf{G}_j(\mathbf{h}(t_\gamma))\mathbf{C}\hat{\mathbf{x}}_{\mathbf{r}}(\mathbf{x_r}(t_\gamma))\big)-\tilde{\mathbf{B}}_{\mathbf{r}}(\mathbf{x_r})\mathbf{r}. \qquad (19)\end{aligned}$$

The control objective is to design the feedback gains $\mathbf{F}_j(\mathbf{h}(t_\gamma))$ and $\mathbf{G}_j(\mathbf{h}(t_\gamma))$, and the membership functions for the IT2 SDOF polynomial fuzzy controller (12) for the realization of the tracking control such that the tracking error $\hat{\mathbf{e}}$ defined in (7) is characterized by H_∞ performance with the consideration of system stability.

In order to adopt the Lyapunov approach to develop the stability conditions, we define $0<\mathbf{X}(\tilde{\mathbf{x}})=\mathbf{X}(\tilde{\mathbf{x}})^T\in\Re^{N\times N}$, $\tilde{\mathbf{x}}=(x_{j_1},x_{j_2},\ldots,x_{j_o},x_{r_{k_1}},x_{r_{k_2}},\ldots,x_{r_{k_s}})$. The row indices $\mathbf{J}=\{j_1,j_2,\ldots,j_o\}$ and $\mathbf{K}=\{k_1,k_2,\ldots,k_s\}$ are the row indicates that the entire row of $\mathbf{B}_i(\mathbf{x})$ and $\mathbf{B}_{\mathbf{r}}(\mathbf{x_r})$ are all zeros, respectively, [16]. Inspired by the work in [9], [15], we choose

$$\mathbf{X}(\tilde{\mathbf{x}})=\begin{bmatrix}\mathbf{X}_{11} & \mathbf{0}\\ \mathbf{0} & \mathbf{X}_{22}(\tilde{\mathbf{x}})\end{bmatrix} \qquad (20)$$

where $\mathbf{X}_{11}\in\Re^{q\times q}$ and $\mathbf{X}_{22}(\tilde{\mathbf{x}})\in\Re^{(N-q)\times(N-q)}$. As $\mathbf{X}(\tilde{\mathbf{x}})$ is required to be positive definite, it implies that the inverse of $\mathbf{X}_{11}$, $\mathbf{X}_{22}(\tilde{\mathbf{x}})$ and $\mathbf{X}(\tilde{\mathbf{x}})$ exist. In addition, we define

$$\mathbf{\Gamma}=[\mathbf{C}^T(\mathbf{C}\mathbf{C}^T)^{-1}\quad \mathrm{ortc}(\mathbf{C}^T)], \qquad (21)$$

where $\mathbf{\Gamma}\in\Re^{N\times N}$ and $\mathrm{ortc}(\mathbf{C}^T)$ denotes the orthogonal complement of $\mathbf{C}^T$ [9], [15]. Consequently, we have

$$\mathbf{C}\mathbf{\Gamma}=[\mathbf{I}_q\quad \mathbf{0}] \qquad (22)$$

where $\mathbf{I}_q\in\Re^{q\times q}$ is the identity matrix. To facilitate the stability analysis, we define an augment vector as $\hat{\mathbf{v}}$ and

$$\hat{\mathbf{v}}=\mathbf{\Gamma}^{-1}\hat{\mathbf{e}}. \qquad (23)$$

From (23), dynamics of $\hat{\mathbf{v}}$ can be represented as follows:

$$\begin{aligned}\dot{\hat{\mathbf{v}}} &= \sum_{i=1}^{p}\sum_{j=1}^{c}\tilde{w}_i(\mathbf{x})\tilde{m}_j(\mathbf{y}(t_\gamma))\big(\mathbf{\Gamma}^{-1}\tilde{\mathbf{A}}_i(\mathbf{x})\mathbf{\Gamma}\mathbf{X}(\tilde{\mathbf{x}})\mathbf{X}^{-1}(\tilde{\mathbf{x}})\mathbf{\Gamma}^{-1}\hat{\mathbf{e}}\\&+\mathbf{\Gamma}^{-1}\tilde{\mathbf{B}}_i(\mathbf{x})\mathbf{F}_j(\mathbf{h}(t_\gamma))\mathbf{C}\mathbf{\Gamma}\mathbf{X}(\tilde{\mathbf{x}})\mathbf{X}^{-1}(\tilde{\mathbf{x}})\mathbf{\Gamma}^{-1}\hat{\mathbf{e}}(t_\gamma)\big)\\&+\sum_{i=1}^{p}\sum_{j=1}^{c}\tilde{w}_i(\mathbf{x})\tilde{m}_j(\mathbf{y}(t_\gamma))\big(\mathbf{\Gamma}^{-1}((\tilde{\mathbf{A}}_i(\mathbf{x})-\tilde{\mathbf{A}}_{\mathbf{r}}(\mathbf{x_r}))\\&\times\mathbf{\Gamma}\mathbf{X}(\tilde{\mathbf{x}})\mathbf{X}^{-1}(\tilde{\mathbf{x}})\mathbf{\Gamma}^{-1}\hat{\mathbf{x}}_{\mathbf{r}}(\mathbf{x_r})+\mathbf{\Gamma}^{-1}\tilde{\mathbf{B}}_i(\mathbf{x})\mathbf{G}_j(\mathbf{h}(t_\gamma))\\&\times\mathbf{C}\mathbf{\Gamma}\mathbf{X}(\tilde{\mathbf{x}})\mathbf{X}^{-1}(\tilde{\mathbf{x}})\mathbf{\Gamma}^{-1}\hat{\mathbf{x}}_{\mathbf{r}}(\mathbf{x_r}(t_\gamma))\big)-\mathbf{\Gamma}^{-1}\tilde{\mathbf{B}}_{\mathbf{r}}(\mathbf{x_r})\mathbf{r}. \quad (24)\end{aligned}$$

From the definition of $\mathbf{\Gamma}$ in (21), we can simplify $\mathbf{F}_j(\mathbf{h}(t_\gamma))\mathbf{C}\mathbf{\Gamma}\mathbf{X}(\tilde{\mathbf{x}})$ and $\mathbf{G}_j(\mathbf{h}(t_\gamma))\mathbf{C}\mathbf{\Gamma}\mathbf{X}(\tilde{\mathbf{x}})$ as

$$\mathbf{F}_j(\mathbf{h}(\mathbf{t}_\gamma))\mathbf{C}\mathbf{\Gamma}\mathbf{X}(\tilde{\mathbf{x}})=[\mathbf{M}_j(\mathbf{h}(t_\gamma))\quad \mathbf{0}], \qquad (25)$$
$$\mathbf{G}_j(\mathbf{h}(\mathbf{t}_\gamma))\mathbf{C}\mathbf{\Gamma}\mathbf{X}(\tilde{\mathbf{x}})=[\mathbf{N}_j(\mathbf{h}(t_\gamma))\quad \mathbf{0}]. \qquad (26)$$

It follows from (24) that

$$\dot{\hat{\mathbf{v}}}=\sum_{i=1}^{p}\sum_{j=1}^{c}\tilde{w}_i(\mathbf{x})\tilde{m}_j(\mathbf{y}(t_\gamma))\Phi_{ij}(\mathbf{x},\mathbf{x_r})\mathbf{z} \qquad (27)$$

where $\Phi_{ij}(\mathbf{x},\mathbf{x_r})=[\Phi_{ij}^{(1)}(\mathbf{x},\mathbf{x_r})\quad \Phi_{ij}^{(2)}(\mathbf{x},\mathbf{x_r})\quad \Phi_{ij}^{(3)}(\mathbf{x},\mathbf{x_r})\quad \Phi_{ij}^{(4)}(\mathbf{x},\mathbf{x_r})\quad \Phi_{ij}^{(5)}(\mathbf{x},\mathbf{x_r})]$, $\Phi_{ij}^{(1)}(\mathbf{x},\mathbf{x_r})=\mathbf{\Gamma}^{-1}\tilde{\mathbf{A}}_i(\mathbf{x})\mathbf{\Gamma}\mathbf{X}(\tilde{\mathbf{x}})$, $\Phi_{ij}^{(2)}(\mathbf{x},\mathbf{x_r})=\mathbf{\Gamma}^{-1}(\tilde{\mathbf{A}}_i(\mathbf{x})-\tilde{\mathbf{A}}_{\mathbf{r}}(\mathbf{x_r}))\mathbf{\Gamma}\mathbf{X}(\tilde{\mathbf{x}})$, $\Phi_{ij}^{(3)}(\mathbf{x},\mathbf{x_r})=\mathbf{\Gamma}^{-1}\tilde{\mathbf{B}}_i(\mathbf{x})[\mathbf{M}_j(\mathbf{h}(t_\gamma))\quad \mathbf{0}]$, $\Phi_{ij}^{(4)}(\mathbf{x},\mathbf{x_r})=\mathbf{\Gamma}^{-1}\tilde{\mathbf{B}}_i(\mathbf{x})[\mathbf{N}_j(\mathbf{h}(t_\gamma))\quad \mathbf{0}]$, $\Phi_{ij}^{(5)}(\mathbf{x},\mathbf{x_r})=-\mathbf{\Gamma}^{-1}\tilde{\mathbf{B}}_{\mathbf{r}}(\mathbf{x_r})$, $\mathbf{z}=\begin{bmatrix}\mathbf{z}_1^T & \mathbf{z}_2^T & \mathbf{z}_3^T & \mathbf{z}_4^T & \mathbf{z}_5^T\end{bmatrix}^T$, $\mathbf{z}_1=\mathbf{X}(\tilde{\mathbf{x}})^{-1}\hat{\mathbf{v}}(t)$, $\mathbf{z}_2=\mathbf{X}(\tilde{\mathbf{x}})^{-1}\mathbf{\Gamma}^{-1}\hat{\mathbf{x}}_{\mathbf{r}}$, $\mathbf{z}_3=\mathbf{X}(\tilde{\mathbf{x}})^{-1}\hat{\mathbf{v}}(t_\gamma)$, $\mathbf{z}_4=\mathbf{X}(\tilde{\mathbf{x}})^{-1}\mathbf{\Gamma}^{-1}\hat{\mathbf{x}}_{\mathbf{r}}(\mathbf{x_r}(t_\gamma))$ and $\mathbf{z}_5=\mathbf{r}$.

To investigate the stability of (27), the following Lyapunov-Krasovskii functional is adopted:

$$V(t)=\hat{\mathbf{v}}^T\mathbf{X}(\tilde{\mathbf{x}})^{-1}\hat{\mathbf{v}}+\int_{-h_s}^{0}\int_{t+\sigma}^{t}\dot{\hat{\mathbf{v}}}(\varphi)^T\mathbf{R}\dot{\hat{\mathbf{v}}}(\varphi)d\varphi d\sigma \quad (28)$$

where $0<\mathbf{R}=\mathbf{R}^T\in\Re^{N\times N}$.

By taking the derivative of $V(t)$, we have

$$\begin{aligned}\dot{V}(t)&=\dot{\hat{\mathbf{v}}}^T\mathbf{X}(\tilde{\mathbf{x}})^{-1}\hat{\mathbf{v}}+\hat{\mathbf{v}}^T\mathbf{X}(\tilde{\mathbf{x}})^{-1}\dot{\hat{\mathbf{v}}}+\hat{\mathbf{v}}^T\frac{d\mathbf{X}(\tilde{\mathbf{x}})^{-1}}{dt}\hat{\mathbf{v}}(t)\\&+h_s\dot{\hat{\mathbf{v}}}^T\mathbf{R}\dot{\hat{\mathbf{v}}}-\int_{t-h_s}^{t}\dot{\hat{\mathbf{v}}}(\varphi)^T\mathbf{R}\dot{\hat{\mathbf{v}}}(\varphi)d\varphi. \qquad (29)\end{aligned}$$

Remark 1: It is defined that $\mathbf{J}=\{j_1,j_2,\ldots,j_o\}$ is the set of row numbers that the entire row of $\mathbf{B}_i(\mathbf{x})$ for all i and $\mathbf{K}=\{k_1,k_2,\ldots,k_s\}$ is the set of row numbers that the entire row of $\mathbf{B}_{\mathbf{r}}(\mathbf{x_r})$ are all zeros. Defining $\tilde{\mathbf{x}}=(x_{j_1},x_{j_2},\ldots,x_{j_o},x_{r_{k_1}},x_{r_{k_2}},\ldots,x_{r_{k_s}})$ as before, it obtains that $\frac{\partial\mathbf{X}(\tilde{\mathbf{x}})^{-1}}{\partial x_g}=-\mathbf{X}(\tilde{\mathbf{x}})^{-1}\frac{\partial\mathbf{X}(\tilde{\mathbf{x}})}{\partial x_g}\mathbf{X}(\tilde{\mathbf{x}})^{-1}$ and $\frac{d\mathbf{X}(\tilde{\mathbf{x}})^{-1}}{dt}=\sum_{k=1}^{n}\big(\frac{\partial\mathbf{X}(\tilde{\mathbf{x}})^{-1}}{\partial x_k}\frac{dx_k}{dt}+\frac{\partial\mathbf{X}(\tilde{\mathbf{x}})^{-1}}{\partial x_{r_k}}\frac{dx_{r_k}}{dt}\big)=-\sum_{g\in\mathbf{J}}\mathbf{X}(\tilde{\mathbf{x}})^{-1}\big(\frac{\partial\mathbf{X}(\tilde{\mathbf{x}})}{\partial x_g}\sum_{i=1}^{p}\tilde{w}_i\mathbf{A}_i^{(g)}(\mathbf{x})\hat{\mathbf{x}}(\mathbf{x})\big)\mathbf{X}(\tilde{\mathbf{x}})^{-1}$ - $\sum_{g\in\mathbf{K}}\mathbf{X}(\tilde{\mathbf{x}})^{-1}\big(\frac{\partial\mathbf{X}(\tilde{\mathbf{x}})^{-1}}{\partial x_{r_g}}\mathbf{A}_r^{(g)}(\mathbf{x_r})\hat{\mathbf{x}}_{\mathbf{r}}(\mathbf{x_r})\big)\mathbf{X}(\tilde{\mathbf{x}})^{-1}$ [16], $\mathbf{A}_i^{(g)}(\mathbf{x})$ and $\mathbf{A}_r^{(g)}(\mathbf{x_r})$ denote the g-th row of $\mathbf{A}_i(\mathbf{x})$ and $\mathbf{A}_r(\mathbf{x_r})$, respectively.

Before proceeding further, the following lemma is introduced to deal with the integral term in (29).

Lemma 1 (Jensen's Inequality): With $\mathbf{b}(\varphi)=\dot{\hat{\mathbf{v}}}(\varphi)\in\Re^N$, $\mathbf{R}>0\in\Re^{N\times N}$ and $\tau>0$, the following inequality always holds [41]:

$$\begin{aligned}&-\int_{t-\tau}^{t}\mathbf{b}(\varphi)^T\mathbf{R}\mathbf{b}(\varphi)d\varphi\\&\le-\frac{1}{\tau}(\hat{\mathbf{v}}(t)-\hat{\mathbf{v}}(t-\tau))^T\mathbf{R}(\hat{\mathbf{v}}(t)-\hat{\mathbf{v}}(t-\tau)). \qquad (30)\end{aligned}$$

Through adopting Lemma 1, when $\tau\le h_s$, we have

$$\begin{aligned}&-\frac{1}{\tau}(\hat{\mathbf{v}}(t)-\hat{\mathbf{v}}(t-\tau))^T\mathbf{R}(\hat{\mathbf{v}}(t)-\hat{\mathbf{v}}(t-\tau))\le\\&-\frac{1}{h_s}(\hat{\mathbf{v}}(t)-\hat{\mathbf{v}}(t-\tau))^T\mathbf{R}(\hat{\mathbf{v}}(t)-\hat{\mathbf{v}}(t-\tau)). \qquad (31)\end{aligned}$$

Applying Lemma 1 to the integral term in (29), combining with (31) and using the fact that $\mathbf{z}_1 = \mathbf{X}(\tilde{\mathbf{x}})^{-1}\hat{\mathbf{v}}$, we have

$$\begin{aligned}\dot{V}(t) \leq\ & \mathbf{z}^T \sum_{i=1}^{p}\sum_{j=1}^{c} \tilde{w}_i(\mathbf{x})\tilde{m}_j(\mathbf{y}(t_\gamma))\Phi_{ij}^T(\mathbf{x},\mathbf{x_r})\mathbf{z}_1 \\ & + \mathbf{z}_1^T \sum_{i=1}^{p}\sum_{j=1}^{c} \tilde{w}_i(\mathbf{x})\tilde{m}_j(\mathbf{y}(t_\gamma))\Phi_{i,j}(\mathbf{x},\mathbf{x_r})\mathbf{z} \\ & + \hat{\mathbf{v}}^T \frac{d\mathbf{X}(\tilde{\mathbf{x}})^{-1}}{dt}\hat{\mathbf{v}} + h_s \mathbf{z}^T \big(\sum_{i=1}^{p}\sum_{j=1}^{c} \tilde{w}_i(\mathbf{x})\tilde{m}_j(\mathbf{y}(t_\gamma)) \\ & \times \Phi_{ij}^T(\mathbf{x},\mathbf{x_r})\mathbf{R} \sum_{i=1}^{p}\sum_{j=1}^{c} \tilde{w}_i(\mathbf{x})\tilde{m}_j(\mathbf{y}(t_\gamma))\Phi_{i,j}(\mathbf{x},\mathbf{x_r})\big)\mathbf{z} \\ & - \frac{1}{h_s}(\hat{\mathbf{v}}(t) - \hat{\mathbf{v}}((t_\gamma))^T \mathbf{R}(\hat{\mathbf{v}}(t) - \hat{\mathbf{v}}(t_\gamma)). \end{aligned} \tag{32}$$

To facilitate the stability analysis in matrix form, the term $-\frac{1}{h_s}(\hat{\mathbf{v}}(t) - \hat{\mathbf{v}}(t_\gamma)^T \mathbf{R}(\hat{\mathbf{v}}(t) - \hat{\mathbf{v}}(t_\gamma))$ in (32) is expressed as

$$\sum_{i=1}^{p}\sum_{j=1}^{c} \tilde{w}_i(\mathbf{x})\tilde{m}_j(\mathbf{y}(t_\gamma))\mathbf{z}^T\mathbf{\Lambda}\mathbf{z} \tag{33}$$

where

$$\mathbf{\Lambda} = \begin{bmatrix} -\frac{1}{h_s}\mathbf{Z} & \mathbf{0} & \frac{1}{h_s}\mathbf{Z} & \mathbf{0} & \mathbf{0} \\ \mathbf{0} & \mathbf{0} & \mathbf{0} & \mathbf{0} & \mathbf{0} \\ \frac{1}{h_s}\mathbf{Z} & \mathbf{0} & -\frac{1}{h_s}\mathbf{Z} & \mathbf{0} & \mathbf{0} \\ \mathbf{0} & \mathbf{0} & \mathbf{0} & \mathbf{0} & \mathbf{0} \\ \mathbf{0} & \mathbf{0} & \mathbf{0} & \mathbf{0} & \mathbf{0} \end{bmatrix}, \tag{34}$$

in which $\mathbf{Z} = \mathbf{X}(\tilde{\mathbf{x}})\mathbf{R}\mathbf{X}(\tilde{\mathbf{x}}) \in \Re^{N\times N}$.

To introduce the H_∞ performance into the analysis, the terms $\mathbf{z}^T \sum_{i=1}^{p}\sum_{j=1}^{c} \tilde{w}_i(\mathbf{x})\tilde{m}_j(\mathbf{y}(t_\gamma))\Phi_{ij}^T(\mathbf{x},\mathbf{x_r})\mathbf{z}_1 + \mathbf{z}_1 \sum_{i=1}^{p}\sum_{j=1}^{c} \tilde{w}_i(\mathbf{x})\tilde{m}_j(\mathbf{y}(t_\gamma))\Phi_{i,j}^T(\mathbf{x},\mathbf{x_r})\mathbf{z} + \hat{\mathbf{v}}^T \frac{d\mathbf{X}(\tilde{\mathbf{x}})^{-1}}{dt}\hat{\mathbf{v}}$ in (32) can be rewritten as

$$\begin{aligned}& \sum_{i=1}^{p}\sum_{j=1}^{c} w_i(\mathbf{x})m_j(\mathbf{y}(t_\gamma))\mathbf{z}^T\mathbf{\Delta}_{ij}(\mathbf{x},\mathbf{x_r})\mathbf{z} - \mathbf{z}_1^T\mathbf{z}_1 - \mathbf{z}_3^T\mathbf{z}_3 \\ & + \sigma_1\mathbf{z}_2^T\mathbf{z}_2 + \sigma_2\mathbf{z}_4^T\mathbf{z}_4 + \sigma_3\mathbf{z}_5^T\mathbf{z}_5 \end{aligned} \tag{35}$$

where

$$\mathbf{\Delta}_{ij}(\mathbf{x},\mathbf{x_r}) = \begin{bmatrix} \mathbf{\Delta}_{ij}^{(11)}(\mathbf{x},\mathbf{x_r}) & * & * & * & * \\ \mathbf{\Phi}_{ij}^{(2)}(\mathbf{x},\mathbf{x_r})^T & -\sigma_1\mathbf{I} & \mathbf{0} & \mathbf{0} & \mathbf{0} \\ \mathbf{\Phi}_{ij}^{(3)}(\mathbf{x},\mathbf{x_r})^T & \mathbf{0} & \mathbf{I} & \mathbf{0} & \mathbf{0} \\ \mathbf{\Phi}_{ij}^{(4)}(\mathbf{x},\mathbf{x_r})^T & \mathbf{0} & \mathbf{0} & -\sigma_2\mathbf{I} & \mathbf{0} \\ \mathbf{\Phi}_{ij}^{(5)}(\mathbf{x},\mathbf{x_r})^T & \mathbf{0} & \mathbf{0} & \mathbf{0} & -\sigma_3\mathbf{I} \end{bmatrix}, \tag{36}$$

The first element $\mathbf{\Delta}_{ij}^{(11)}(\mathbf{x},\mathbf{x_r})$ in the above matrix is defined as: $\mathbf{\Delta}_{ij}^{(11)}(\mathbf{x},\mathbf{x_r}) = \mathbf{\Phi}_{ij}^{(1)}(\mathbf{x},\mathbf{x_r}) + \mathbf{\Phi}_{ij}^{(1)}(\mathbf{x},\mathbf{x_r})^T - \sum_{g\in\mathbf{J}} \frac{\partial\mathbf{X}(\tilde{\mathbf{x}})}{\partial x_g}\mathbf{A}_i^{(g)}(\mathbf{x})\hat{\mathbf{x}}(\mathbf{x}) - \sum_{g\in\mathbf{K}} \frac{\partial\mathbf{X}(\tilde{\mathbf{x}})}{\partial x_{g_k}}\mathbf{A}_r^{(g)}(\mathbf{x})\hat{\mathbf{x}}_r(\mathbf{x_r}) + \mathbf{I}$; $\mathbf{I}$ is the identify matrix of compatible dimensions; the other elements in the first column have already been defined in the context under (27); $\sigma_1 > 0$, $\sigma_2 > 0$ and $\sigma_3 > 0$ are scalars to be determined which are related to the tracking performance characterized by an H_∞ performance index.

Considering the expression of (33) and (35), (32) can be written in a more concise way as follows:

$$\begin{aligned}\dot{V}(t) \leq & \mathbf{z}^T\mathbf{\Theta}(\mathbf{x},\mathbf{x_r})\mathbf{z} - \mathbf{z}_1^T\mathbf{z}_1 - \mathbf{z}_3^T\mathbf{z}_3 \\ & + \sigma_1\mathbf{z}_2^T\mathbf{z}_2 + \sigma_2\mathbf{z}_4^T\mathbf{z}_4 + \sigma_3\mathbf{z}_5^T\mathbf{z}_5 \end{aligned} \tag{37}$$

where

$$\begin{aligned}\mathbf{\Theta}(\mathbf{x},\mathbf{x_r}) = & \sum_{i=1}^{p}\sum_{j=1}^{c} \tilde{w}_i(\mathbf{x})\tilde{m}_j(\mathbf{y}(t_\gamma))(\mathbf{\Delta}_{ij}(\mathbf{x},\mathbf{x_r}) + \mathbf{\Lambda}) + \\ & h_s\big(\sum_{i=1}^{p}\sum_{j=1}^{c} \tilde{w}_i(\mathbf{x})\tilde{m}_j(\mathbf{y}(t_\gamma))\Phi_{ij}^T(\mathbf{x},\mathbf{x_r})\mathbf{R} \\ & \times \sum_{i=k}^{p}\sum_{j=l}^{c} \tilde{w}_k(\mathbf{x})\tilde{m}_l(\mathbf{y}(t_\gamma))\Phi_{k,l}(\mathbf{x},\mathbf{x_r})\big). \end{aligned} \tag{38}$$

Once $\mathbf{\Theta}(\mathbf{x},\mathbf{x_r}) < 0$ is guaranteed, then the following inequality can be obtained:

$$\dot{V}(t) \leq -\mathbf{z}_1^T\mathbf{z}_1 - \mathbf{z}_3^T\mathbf{z}_3 + \sigma_1\mathbf{z}_2^T\mathbf{z}_2 + \sigma_2\mathbf{z}_4^T\mathbf{z}_4 + \sigma_3\mathbf{z}_5^T\mathbf{z}_5. \tag{39}$$

Considering the termination time of control t_f [8], [15] and taking integration on both sides of (39) with respect to time t, we obtain the following H_∞ performance:

$$\frac{\int_0^{t_f}(\mathbf{z}_1^T\mathbf{z}_1 + \mathbf{z}_3^T\mathbf{z}_3) - \mathbf{V}(0)}{\int_0^{t_f}(\sigma_1\mathbf{z}_2^T\mathbf{z}_2 + \sigma_2\mathbf{z}_4^T\mathbf{z}_4 + \sigma_3\mathbf{z}_5^T\mathbf{z}_5)} \leq 1. \tag{40}$$

Remark 2: In (40), $\mathbf{z}_1$ and $\mathbf{z}_3$ relate to the values of $\hat{\mathbf{v}}(t)$ and $\hat{\mathbf{v}}(t_\gamma)$, respectively, which are further related to the tracking error $\hat{\mathbf{e}}(t)$ and $\hat{\mathbf{e}}(t_\gamma)$. It can be seen that smaller values of σ_1, σ_2 and σ_3 will reduce the value of $\int_0^{t_f}(\mathbf{z}_1^T\mathbf{z}_1 + \mathbf{z}_3^T\mathbf{z}_3)$, which leads to an improved H_∞ performance. In this paper, finding the minimum values of σ_1, σ_2 and σ_3 will be formulated as the generalized eigenvalue problem (GEVP).

The above result is based on the satisfaction of the condition: $\mathbf{\Theta}(\mathbf{x},\mathbf{x_r}) < 0$. If Schur complement lemma is applied directly to deal with the last term in (38), $\mathbf{Z}^{-1}$ will be generated and further leads to a non-convex condition. To circumvent this problem, we use the inequality $2\xi\mathbf{X}(\tilde{\mathbf{x}}) - \xi^2\mathbf{Z} \leq \mathbf{X}(\tilde{\mathbf{x}})\mathbf{Z}^{-1}\mathbf{X}(\tilde{\mathbf{x}})$ [14], where ξ is a scalar chosen by the user, to render it to a convex condition. Adopting the inequality, $\mathbf{\Theta}(\mathbf{x},\mathbf{x_r}) < 0$ is implied by the following condition:

$$\sum_{i=1}^{p}\sum_{j=1}^{c} \tilde{w}_i(\mathbf{x})\tilde{m}_j(\mathbf{y}(t_\gamma))\mathbf{\Xi}_{ij}(\mathbf{x},\mathbf{x_r}) < 0 \tag{41}$$

where

$$\mathbf{\Xi}_{ij}(\mathbf{x},\mathbf{x_r}) = \begin{bmatrix} \mathbf{\Delta}_{ij}(\mathbf{x},\mathbf{x_r}) + \mathbf{\Lambda} & * \\ h_s\mathbf{\Phi}_{ij}(\mathbf{x},\mathbf{x_r}) & -h_s(2\xi\mathbf{X}(\tilde{\mathbf{x}}) - \xi^2\mathbf{Z}) \end{bmatrix}. \tag{42}$$

Consequently, the satisfaction of the condition: $\mathbf{\Xi}_{ij}(\mathbf{x},\mathbf{x_r}) < 0$ for all i and j can make sure that $\mathbf{\Theta}(\mathbf{x},\mathbf{x_r}) < 0$. The results for the stability analysis and H_∞ performance are summarized in the following theorem.

Theorem 1: Considering the IT2 SDOF PFMB control system, which is formed by a nonlinear plant represented by the IT2 polynomial fuzzy model (4) and the IT2 SDOF polynomial fuzzy controller (12) connected in a closed loop, its system states are driven to follow those of the reference model (6) subject to the H_∞ performance (40) if there exist scalars $\sigma_1 > 0$, $\sigma_2 > 0$, $\sigma_3 > 0$, and polynomial matrices $\mathbf{M}_j(\mathbf{h}(t_\gamma)) \in \Re^{m\times q}$, $\mathbf{N}_j(\mathbf{h}(t_\gamma)) \in \Re^{m\times q}$, $\mathbf{X}(\tilde{\mathbf{x}}) = \mathbf{X}(\tilde{\mathbf{x}})^T \in \Re^{N\times N}$ with the structure given in (20), $\mathbf{Z} = \mathbf{Z}^T \in \Re^{N\times N}$, $j = 1, 2, \ldots, c$, such that the following GEVP is feasible:

$$\begin{aligned}&\min \sigma_1 + \sigma_2 + \sigma_3 \text{ subject to}\\ &\sigma_1 > 0; \sigma_2 > 0; \sigma_3 > 0; \nu_1^T(\mathbf{X}(\tilde{\mathbf{x}}) - \varepsilon_1(\tilde{\mathbf{x}})\mathbf{I})\nu_1 \text{ is SOS;}\\ &\nu_1^T(\mathbf{Z} - \varepsilon_2(\tilde{\mathbf{x}})\mathbf{I})\nu_1 \text{ is SOS;} -\nu_2^T(\mathbf{\Xi}_{ij}(\mathbf{x},\mathbf{x_r}) + \varepsilon_3(\mathbf{x},\mathbf{x_r})\mathbf{I})\nu_2\\ &\text{is SOS}, i = 1, 2, \ldots, p; j = 1, 2, \ldots, c \qquad (43)\end{aligned}$$

where $\nu_1 \in \Re^N$ and $\nu_2 \in \Re^{5N+m}$ are arbitrary vectors independent of $\mathbf{x}$ and $\mathbf{x_r}$; ξ is a predefined scalar; $\varepsilon_1(\tilde{\mathbf{x}}) > 0$ and $\varepsilon_3(\mathbf{x},\mathbf{x_r}) > 0$ are predefined scalar polynomials; $\varepsilon_2(\tilde{\mathbf{x}}) > 0$ is a predefined scalar. The polynomial feedback gains are defined in (25) abd (26).

Remark 3: The stability conditions in Theorem 1 are MFI and thus are conservative.

B. MFD Stability Conditions with H_∞ Performance

The idea of bringing the membership functions into the analysis helps relax the stability condition when the sub-domain information, approximation of $\tilde{w}_i(\mathbf{x})\tilde{m}_j(\mathbf{y}(t_\gamma))$ and output-state information are considered. To obtain the sub-domain information, the operating domain of $\mathbf{x}$ denoted as Φ is divided into L connected sub-domains according to $\mathbf{x}$ denoted as Φ_l, l = 1, 2, ..., L such that $\Phi = \bigcup_{l=1}^{L}\Phi_l$. Let us define $\tilde{h}_{ij}(\mathbf{x},\mathbf{y}(t_\gamma)) \equiv \tilde{w}_i(\mathbf{x})\tilde{m}_j(\mathbf{y}(t_\gamma))$ to make the analysis more concise. An approximation function $\hat{h}_{ijl}(\mathbf{x})$ of the l-th operating sub-domain for $\mathbf{x} \in \Phi_l$ is chosen to estimate $\tilde{h}_{ij}(\mathbf{x},\mathbf{y}(t_\gamma))$ that the constant approximation error δ_{ijl} in the l-th operating sub-domain satisfies

$$0 \le \tilde{h}_{ij}(\mathbf{x},\mathbf{y}(t_\gamma)) - \hat{h}_{ijl}(\mathbf{x}) \le \delta_{ijl},\ \forall\, l, \mathbf{x} \in \Phi_l. \qquad (44)$$

To take the output-state information into account, it is assumed that the system output $\mathbf{y}$ is elementwisely lower bounded by $\underline{\mathbf{y}}_l \in \Re^q$ and upper bounded by $\overline{\mathbf{y}}_l \in \Re^q$ in the l-th sub-operating domain. As a results, we have:

$$(\mathbf{y} - \underline{\mathbf{y}}_l)^T\mathbf{D}(\overline{\mathbf{y}}_l - \mathbf{y})\mathbf{S}_l(\mathbf{y}) \ge 0,\ \forall\, l, \mathbf{x} \in \Phi_l, \qquad (45)$$

where $\mathbf{D} = \text{diag}\{d_1, d_2, \ldots, d_q\} \in \Re^{q\times q}$ is a diagonal matrix whose elements are either 0 or 1. When $d_r = 1$, r = 1, 2,..., q, the output-state information of y_r is included, otherwise, not included; $0 \le \mathbf{S}_l(\mathbf{y}) = \mathbf{S}_l^T(\mathbf{y}) \in \Re^{(5N+m)\times(5N+m)}$, l = 1, 2, ..., L, is a slack polynomial matrix to be determined.

Considering (44) and (45), and defining slack matrix variable $0 \le \mathbf{Y}_{ijl}(\mathbf{x},\mathbf{x_r}) = \mathbf{Y}_{ijl}(\mathbf{x},\mathbf{x_r})^T \in \Re^{(5N+m)\times(5N+m)}$ which satisfies $\mathbf{Y}_{ijl}(\mathbf{x},\mathbf{x_r}) \ge \mathbf{\Xi}_{ij}(\mathbf{x},\mathbf{x_r})$, all the membership function information can be added to (41) such that we have

$$\begin{aligned}&\sum_{i=1}^{p}\sum_{j=1}^{c}\tilde{h}_{ij}(\mathbf{x},\mathbf{y}(t_\gamma))\mathbf{\Xi}_{ij}\\ &= \sum_{i=1}^{p}\sum_{j=1}^{c}(\hat{h}_{ijl}(\mathbf{x}) + \tilde{h}_{ij}(\mathbf{x},\mathbf{y}(t_\gamma)) - \hat{h}_{ijl}(\mathbf{x}))\mathbf{\Xi}_{ij}(\mathbf{x},\mathbf{x_r})\\ &\le \sum_{i=1}^{p}\sum_{j=1}^{c}(\hat{h}_{ijl}(\mathbf{x})\mathbf{\Xi}_{ij}(\mathbf{x},\mathbf{x_r}) + \delta_{ijl}\mathbf{Y}_{ijl}(\mathbf{x},\mathbf{x_r}))\\ &\quad + (\mathbf{y} - \underline{\mathbf{y}}_l)^T\mathbf{D}(\overline{\mathbf{y}}_l - \mathbf{y})\mathbf{S}_l(\mathbf{y}),\ \forall\, l, \mathbf{x} \in \Phi_l. \qquad (46)\end{aligned}$$

When the right hand side of (46) is negative definite, the system states of the IT2 SDOF PFMB control system are driven to follow those of the reference model (6) subject to the H_∞ performance (40). The above MFD stability analysis results are summarized as in the following theorem.

Theorem 2: Considering the IT2 SDOF PFMB control system, which is formed by a nonlinear plant represented by the IT2 polynomial fuzzy model (4) and the IT2 SDOF polynomial fuzzy controller (12) connected in a closed loop, its system states are driven to follow those of the reference model (6) subject to the H_∞ performance (40) if there exist polynomial matrices $\mathbf{S}_l(\mathbf{y}) = \mathbf{S}_l(\mathbf{y})^T \in \Re^{(5N+m)\times(5N+m)}$, $\mathbf{M}_j(\mathbf{h}(t_\gamma)) \in \Re^{m\times q}$, $\mathbf{N}_j(\mathbf{h}(t_\gamma)) \in \Re^{m\times q}$, $\mathbf{Z} = \mathbf{Z}^T \in \Re^{N\times N}$, $\mathbf{X}(\tilde{\mathbf{x}}) = \mathbf{X}(\tilde{\mathbf{x}})^T \in \Re^{N\times N}$, $\mathbf{Y}_{ijl}(\mathbf{x},\mathbf{x_r}) = \mathbf{Y}_{ijl}(\mathbf{x},\mathbf{x_r})^T \in \Re^{(5N+m)\times(5N+m)}$, i = 1, 2, ..., p, j = 1, 2, ..., c, l = 1, 2, ..., L, such that the following SOS-based GEVP conditions are satisfied:

$$\begin{aligned}&\min \sigma_1 + \sigma_2 + \sigma_3 \text{ subject to}\\ &\sigma_1 > 0; \sigma_2 > 0; \sigma_3 > 0; \rho^T(\mathbf{S}_l(\mathbf{y}) - \varepsilon_1(\mathbf{y})\mathbf{I})\rho \text{ is SOS}, \forall\, l;\\ &\rho^T(\mathbf{Y}_{ijl}(\mathbf{x},\mathbf{x_r}) - \varepsilon_3(\mathbf{x},\mathbf{x_r})\mathbf{I})\rho \text{ is SOS}, \forall\, i, j, l;\\ &\rho^T(\mathbf{Y}_{ijl}(\mathbf{x},\mathbf{x_r}) - \mathbf{\Xi}_{ij}(\mathbf{x},\mathbf{x_r}) - \varepsilon_4(\mathbf{x},\mathbf{x_r})\mathbf{I})\rho \text{ is SOS},\\ &\forall\, i, j, l; \nu^T(\mathbf{X}(\tilde{\mathbf{x}}) - \varepsilon_2(\tilde{\mathbf{x}})\mathbf{I})\nu \text{ is SOS;}\\ &-\rho^T\Big(\sum_{i=1}^{p}\sum_{j=1}^{c}(\hat{h}_{ijl}(\mathbf{x})\mathbf{\Xi}_{ij}(\mathbf{x},\mathbf{x_r}) + \delta_{ijl}\mathbf{Y}_{ijl}(\mathbf{x},\mathbf{x_r})) +\\ &(\mathbf{y} - \underline{\mathbf{y}}_l)^T\mathbf{D}(\overline{\mathbf{y}}_l - \mathbf{y})\mathbf{S}_l(\mathbf{y}) + \varepsilon_5(\mathbf{x},\mathbf{x_r})\mathbf{I}\Big)\rho \text{ is SOS}, \quad \forall\, l\\ &\nu^T(\mathbf{Z} - \varepsilon_6(\tilde{\mathbf{x}})\mathbf{I})\nu \text{ is SOS;}\end{aligned}$$

where $\nu \in \Re^N$ is an arbitrary vector independent of $\mathbf{x}$, $\mathbf{x_r}$ and $\mathbf{y}$, $\rho \in \Re^{5N+m}$ is an arbitrary vector independent of $\mathbf{x}$, $\mathbf{x_r}$ and $\mathbf{y}$, $\hat{h}_{ijl}(\mathbf{x})$ and δ_{ijl} are determined by the upper and lower bounds of the IT2 membership functions; $\mathbf{D} = \text{diag}\{d_1, d_2, \ldots, d_q\} \in \Re^{q\times q}$ is a predefined diagonal matrix; $\varepsilon_1(\mathbf{y}) > 0$, $\varepsilon_2(\tilde{\mathbf{x}}) > 0$, $\varepsilon_3(\mathbf{x},\mathbf{x_r}) > 0$, $\varepsilon_4(\mathbf{x},\mathbf{x_r}) > 0$, $\varepsilon_5(\mathbf{x},\mathbf{x_r}) > 0, \varepsilon_6(\tilde{\mathbf{x}}) > 0$ are predefined scalar polynomials; $\underline{\mathbf{y}}_l$ and $\overline{\mathbf{y}}_l$ are the predefined lower and upper bounds of the system output vector $\mathbf{y}$, respectively, in the l-th operating sub-domain. The polynomial feedback gains are defined in (25) and (26).

Remark 4: Some conditions in Theorem 2 contain the output state vector $\mathbf{y}$. From (5), $\mathbf{y}$ is a function of $\mathbf{x}$, it is thus all conditions in Theorem 2 depending on $\mathbf{x}$ (continuous and sampled versions) only.

In order to obtain the values of $\hat{h}_{ijl}(\mathbf{x})$ and δ_{ijl}, the following analysis steps are adopted:

1) Finding $\dot{\hat{\mathbf{x}}}_{max}$*:* To apply Theorem 2, it needs to determine δ_{ijl} which satisfies the condition (44). In order to determine δ_{ijl}, $\dot{\hat{\mathbf{x}}}_{max}$ needs to be determined first. To obtain $\dot{\hat{\mathbf{x}}}_{max}$ used in (48) and (49), let us recall the definition of $\dot{\hat{\mathbf{x}}}$ in (14), which is $\dot{\hat{\mathbf{x}}} = \mathbf{T}(\mathbf{x})\dot{\mathbf{x}}$. Then the $\dot{\hat{\mathbf{x}}}_{max}$ can be calculated by $\mathbf{T}(\mathbf{x})$ and $\dot{\mathbf{x}}$: $\dot{\hat{\mathbf{x}}}_{max} =$

$\left[\begin{array}{cccc}\max_{\mathbf{x}\in\Phi}(\mathbf{T}_1(\mathbf{x})\dot{\mathbf{x}}) & \max_{\mathbf{x}\in\Phi}(\mathbf{T}_2(\mathbf{x})\dot{\mathbf{x}}) & \cdots & \max_{\mathbf{x}\in\Phi}(\mathbf{T}_N(\mathbf{x})\dot{\mathbf{x}})\end{array}\right]^T$ where $\mathbf{T}_1(\mathbf{x}), \mathbf{T}_2(\mathbf{x}), \ldots, \mathbf{T}_N(\mathbf{x})$ are the row vectors of $\mathbf{T}(\mathbf{x})$ and Φ denotes the operating domain of $\mathbf{x}$ defined in prior.

2) Finding δ_{ijl}: Recalling that $\tilde{h}_{ij}(\mathbf{x}, \mathbf{y}(t_\gamma)) \equiv \tilde{w}_i(\mathbf{x})\tilde{m}_j(\mathbf{y}(t_\gamma))$, it depends on both $\mathbf{x}(t)$ and $\mathbf{y}(t_\gamma)$. When we treat $\mathbf{y}(t_\gamma)$ as an independent variable with $\mathbf{x}(t)$, the information of membership function may not be captured well by δ_{ijl} as $\mathbf{y}(t_\gamma)$ is somewhat related to $\mathbf{x}$ according to the system output defined in (5). If we can estimate $\tilde{m}_j(\mathbf{y}(t_\gamma))$ by $\tilde{m}_j(\mathbf{x})$, then $\tilde{h}_{ij}(\mathbf{x}, \mathbf{y}(t_\gamma))$ can be estimated by $\tilde{w}_i(\mathbf{x})\tilde{m}_j(\mathbf{x})$ which depends on the only variable $\mathbf{x}$. As a result, it could make easy the estimation of δ_{ijl} in (44).

To realize the above estimation, we first find the relationship between $\mathbf{y}(t_\gamma)$ and $\mathbf{y}(t)$ during the sampling period by considering the system output. With (5) and (14), we have

$$\mathbf{y}(t) - \mathbf{y}(t_\gamma) = \int_{t_\gamma}^{t} \dot{\mathbf{y}}(\sigma)d\sigma = \int_{t_\gamma}^{t} \mathbf{C}\dot{\hat{\mathbf{x}}}(\mathbf{x}(\sigma))d\sigma. \quad (47)$$

Denoting $\dot{\hat{\mathbf{x}}}_{max} \in \Re^N$ as a vector of constant values which is the maximum value of $|\dot{\hat{\mathbf{x}}}(\mathbf{x}(t))|$ in the operating domain, i.e., $|\dot{\hat{\mathbf{x}}}(\mathbf{x}(t))| \leq \dot{\hat{\mathbf{x}}}_{max}$, from (47), we can obtain

$$|\mathbf{y}(t) - \mathbf{y}(t_\gamma)| \leq (t - t_\gamma)\mathbf{C}\dot{\hat{\mathbf{x}}}_{max} \leq h_s\mathbf{C}\dot{\hat{\mathbf{x}}}_{max}. \quad (48)$$

From (47) and (48), it follows that

$$\begin{aligned}\mathbf{y}(t_\gamma) &\in [\mathbf{y}(t) - h_s\mathbf{C}\dot{\hat{\mathbf{x}}}_{max}, \quad \mathbf{y}(t) + h_s\mathbf{C}\dot{\hat{\mathbf{x}}}_{max}] \\ &= [\mathbf{C}\hat{\mathbf{x}}(t) - h_s\mathbf{C}\dot{\hat{\mathbf{x}}}_{max}, \quad \mathbf{C}\hat{\mathbf{x}}(t) + h_s\mathbf{C}\dot{\hat{\mathbf{x}}}_{max}]. \quad (49)\end{aligned}$$

The above result is summarized as follows: given any $\mathbf{x}$, assuming that $|\dot{\hat{\mathbf{x}}}(\mathbf{x}(t))| \leq \dot{\hat{\mathbf{x}}}_{max}$ is satisfied, $\mathbf{y}(t_\gamma)$ will be in the range of $[\mathbf{C}\hat{\mathbf{x}}(t) - h_s\mathbf{C}\dot{\hat{\mathbf{x}}}_{max}, \quad \mathbf{C}\hat{\mathbf{x}}(t) + h_s\mathbf{C}\dot{\hat{\mathbf{x}}}_{max}]$. Consequently, from (44), δ_{ijl} can be determined numerically by estimating $\tilde{h}_{ij}(\mathbf{x}, \mathbf{y}(t_\gamma)) - \hat{h}_{ijl}(\mathbf{x})$ for $\mathbf{x} \in \Phi_l$; $\mathbf{y}(t_\gamma) \in [\mathbf{C}\hat{\mathbf{x}}(t) - h_s\mathbf{C}\dot{\hat{\mathbf{x}}}_{max}, \quad \mathbf{C}\hat{\mathbf{x}}(t) + h_s\mathbf{C}\dot{\hat{\mathbf{x}}}_{max}]$ and all l.

IV. Simulation Examples

A. Numerical Example

To verify the stability conditions presented in the previous section, let us consider a nonlinear system subject to uncertainty, which is represented by a three-rule polynomial fuzzy model equipped with IT2 membership functions and $\hat{\mathbf{x}}(\mathbf{x}(t)) = \mathbf{x}(t) = [x_1(t) \quad x_2(t)]^T$,

$$\mathbf{A}_1(x_1(t)) = \begin{bmatrix} 0.59 - 0.12x_1(t) & -7.29 - 1.82x_1(t) \\ 0.01 & -2.85 \end{bmatrix},$$

$$\mathbf{A}_2(x_1(t)) = \begin{bmatrix} 0.02 + 2.25x_1(t) & -4.64 + 0.72x_1(t) \\ 0.35 & -8.56 \end{bmatrix},$$

$$\mathbf{A}_3(x_1(t)) = \begin{bmatrix} 0.73 + 0.45x_1(t) & 8.45 + 2.13x_1(t) \\ 0.26 & -15.43 \end{bmatrix},$$

$$\mathbf{B}_1(x_1(t)) = \begin{bmatrix} 1 + 1.35x_1(t) + 2.33x_1(t)^2 \\ 0 \end{bmatrix},$$

$$\mathbf{B}_2(x_1(t)) = \begin{bmatrix} 8 - 0.62x_1(t) \\ 0 \end{bmatrix}, \quad \mathbf{B}_3(x_1(t)) = \begin{bmatrix} 4 - 0.73x_1(t) + 3.35x_1(t)^2 \\ 0.8 \end{bmatrix}, \mathbf{C} = [1 \quad 0].$$

We have the output $\mathbf{y}(t) = \mathbf{C}\hat{\mathbf{x}}(\mathbf{x}(t)) = x_1(t)$ in this simulation and we will use $x_1(t)$ in this example instead of using $\mathbf{y}(t)$. The membership functions are chosen as $\underline{w}_1(x_1(t)) = 1 - 1/(1 + e^{(-x_1(t)-3.5)})$, $\underline{w}_3(x_1(t)) = 1/(1 + e^{(-x_1(t)+3.5)})$, $\overline{w}_2(x_1(t)) = 1 - \underline{w}_1(x_1(t)) - \underline{w}_3(x_1(t))$; $\overline{w}_1(x_1(t)) = 1 - 1/(1 + e^{(-x_1(t)-2.5)})$, $\overline{w}_3(x_1(t)) = 1/(1 + e^{(-x_1(t)+2.5)})$, $\underline{w}_2(x_1(t)) = 1 - \overline{w}_1(x_1(t)) - \overline{w}_3(x_1(t))$.

A two-rule IT2 SDOF polynomial fuzzy controller is employed to realise the tracking control where the IT2 membership functions are chosen as $\underline{m}_1(x_1(t)) = \{1 \text{ for } x_1(t) < -5.2; \frac{-x_1(t)+4.8}{10} \text{ for } -5.2 \leq x_1(t) \leq 4.8; 0 \text{ for } x_1(t) > 4.8$ and $\overline{m}_1(x_1(t)) = \{1 \text{ for } x_1(t) < -4.8; \frac{-x_1(t)+5.2}{10} \text{ for } -4.8 \leq x_1(t) \leq 5.2; 0 \text{ for } x_1(t) > 5.2\}$, $\overline{m}_2(x_1(t)) = 1 - \underline{m}_1(x_1(t))$, $\underline{m}_2(x_1(t)) = 1 - \overline{m}_1(x_1(t))$, and $\tilde{m}_2(x_1(t)) = 1 - \tilde{m}_1(x_1(t))$. The reference model is chosen as $\mathbf{A_r} = \begin{bmatrix} -1.5 & -1 \\ 0.3 & -8.5 \end{bmatrix}$, $\mathbf{B_r} = \begin{bmatrix} 0 \\ 1 \end{bmatrix}$ and $r(t) = 0.5\sin(0.2t)$.

Considering that the system working in $x_1 \in [-10, 10]$. As $y = x_1$, it suggests that the lower and upper bounds of y is $\underline{y} = -10$ and $\overline{y} = 10$. The sampling period in this simulation is set as $h_s = 0.05$s. Assuming $\dot{x_1}(t) \in [-20 \quad 20]$, the largest variation of x_1 within the sampling period is $\int_t^{t+h_s} x_1(t)dt \leq 20 \times h_s$, which is within domain $[-1 \quad 1]$. It should be noted that this assumption should be verified by simulations. With this information, from Section III-B2, it can be obtained that $y(t_\gamma) \in [x_1(t) - 1, \quad x_1(t) + 1]$. By dividing the operating domain $x_1(t)$ into 15 uniform sub-domains (i.e., L = 15), we have $\underline{y}_l = \underline{x}_{1_l} = -\frac{34}{3} + \frac{4}{3}l$ and $\overline{y}_l = \overline{x}_{1_l} = -10 + \frac{4}{3}l$, l = 1, 2, …, 15, which are the lower and upper bounds of the l-th operating sub-domains of the operating domain, respectively. It is chosen that $\mathbf{D} = 1$.

By applying the stability conditions in Theorem 2, it is chosen that $\varepsilon_1(\mathbf{y}) = \varepsilon_2(\tilde{\mathbf{x}}) = \varepsilon_3(\mathbf{x}, \mathbf{x_r}) = \varepsilon_4(\mathbf{x}, \mathbf{x_r}) = \varepsilon_5(\mathbf{x}, \mathbf{x_r}) = \varepsilon_6(\tilde{\mathbf{x}}) = 0.001$, $\mathbf{X}(\tilde{\mathbf{x}})$ as a polynomial of degree 0; $\mathbf{M}_j(x_1(t_\gamma))$ and $\mathbf{N}_j(x_1(t_\gamma))$, j = 1, 2 are polynomials with monomials in x_1 of degree 0; $\mathbf{S}_l(x_1(t))$ is of degree 0; $\mathbf{X}_{22}(\tilde{\mathbf{x}})$ is of degree 0 which lead to $\mathbf{X}(\tilde{\mathbf{x}})$ a constant matrix with $\tilde{\mathbf{x}}$ as a null vector. The feedback gains are obtained as $\mathbf{F}_1 = -1.1515$, $\mathbf{F}_2 = -7.0323$, $\mathbf{G}_1 = 1.0067 \times 10^{-11}$, $\mathbf{G}_2 = 9.3380 \times 10^{-12}$, and $\mathbf{X} = \begin{bmatrix} 7.7228 \times 10^{-4} & 1.9405 \times 10^{-4} \\ 1.9405 \times 10^{-4} & 1.5048 \times 10^{-3} \end{bmatrix}$. The minimum values of σ_1, σ_2 and σ_3 are obtained as 1.8368, 0.9796 and 1.5697, respectively.

To perform simulation, we choose $\underline{\lambda}_1(x_1(t)) = (\sin(5x_1(t)) + 1)/2$, $\overline{\lambda}_1(x_1(t)) = 1 - \underline{\lambda}_1(x_1(t))$, $\underline{\lambda}_3(x_1(t)) = (\cos(5x_1(t)) + 1)/2$, $\overline{\lambda}_3(x_1(t)) = 1 - \underline{\lambda}_3(x_1(t))$, which act as the uncertainty of the nonlinear plant embedded in the IT2 membership functions to obtain $\tilde{w}_1(x_1(t))$ and $\tilde{w}_3(x_1(t))$. Since $\tilde{w}_2(x_1(t)) = 1 - \tilde{w}_1(x_1(t)) - \tilde{w}_3(x_1(t))$, there is no need to obtain the explicit form of $\underline{\lambda}_2(x_1(t))$ and $\overline{\lambda}_2(x_1(t))$ once $\tilde{w}_1(x_1(t))$ and $\tilde{w}_3(x_1(t))$ are defined.

On the other hand, the type reduction in (11) for the controller are chosen as $\underline{\kappa}_j(x_1(t)) = \overline{\kappa}_j(x_1(t)) = 0.5$, j = 1, 2. By applying the IT2 SDOF polynomial fuzzy controller for tracking control with the initial conditions $\mathbf{x}(0) = [0 \quad 0]$ and

$\mathbf{x_r}(0) = [0.5 \quad 0]$, the simulation results of state response and control signal are shown in Fig. 1, which demonstrate that the tracking errors are sufficiently small.

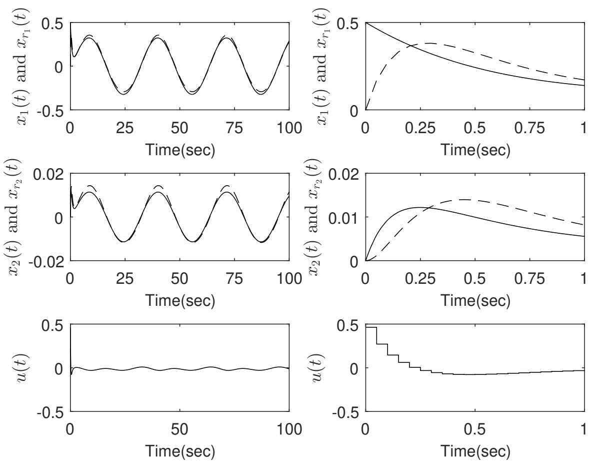

Fig. 1: Tracking control performance for $x_1(t)$ under 15 sub-domains, $\sigma_1 = 1.8368$, $\sigma_2 = 0.9796$ and $\sigma_3 = 1.5697$. Top left: responses of $x_1(t)$ (Dash line) and $x_{r_1}(t)$ (Solid line) from 0 to 100 seconds. Top right: responses of $x_1(t)$ (Dash line) and $x_{r_1}(t)$ (Solid line) from 0 to 1 second. Middle left: responses of $x_2(t)$ (Dash line) and $x_{r_2}(t)$ (Solid line) from 0 to 100 seconds. Middle right: responses of $x_2(t)$ (Dash line) and $x_{r_2}(t)$ (Solid line) from 0 to 1 second. Bottom left:$u(t)$ from 0 to 100 seconds. Bottom right: $u(t)$ from 0 to 1 second.

For comparison purposes, Theorem 1 is applied with $\varepsilon_1(\tilde{\mathbf{x}}) = \varepsilon_2(\tilde{\mathbf{x}}) = \varepsilon_3(\mathbf{x}, \mathbf{x_r}) = 0.001$ and the same degrees of feedback gains and $\tilde{\mathbf{x}}$ used above. However, no feasible solution can be found. It shows that bringing the information of membership functions helps relax the stability analysis results.

B. Inverted Pendulum

An inverted pendulum subject to mass parameters uncertainty is considered that its dynamic equation [18] is:

$$\ddot{\theta}(t) = \frac{g\sin(\theta(t)) - am_pS\dot{\theta}(t)^2\sin(2\theta(t))/2 - a\cos(\theta(t))u(t)}{4S/3 - am_pS\cos^2(\theta(t))} \tag{50}$$

where $\theta(t)$ is the angular displacement of the inverted pendulum, $g = 9.8$ m/s^2, $m_p \in [m_{p_{\min}} \quad m_{p_{\max}}] = [0.5 \quad 1]$ kg is the mass of the pendulum, $M_c \in [M_{c_{\min}} \quad M_{c_{\max}}] = [18 \quad 20]$ kg is the mass of the cart, $a = \frac{1}{m_p+M_c}$, $2S = 1$m is the length of the pendulum, and $u(t)$ is the force applied on the cart. m_p and M_c are treated as the parameter uncertainties. In the fuzzy modeling process, the IT2 membership functions will be used to capture the parameters uncertainty directly and the polynomial fuzzy model will be used to capture the nonlinearity in the system.

Considering $\theta(t) = [\frac{-5\pi}{12}, \frac{5\pi}{12}]$ and $\dot{\theta}(t) = [-4, 4]$, 4 fuzzy rules are used to describe the inverted pendulum by following (1), (2) and (4).

The IT2 polynomial fuzzy model is obtained as $\dot{\mathbf{x}}(t) = \sum_{i=1}^{4} \tilde{w}_i\big(\mathbf{A}_i(\mathbf{x}(t))\hat{\mathbf{x}}(\mathbf{x}(t)) + \mathbf{B}_i(\mathbf{x}(t))u(t)\big)$ and

TABLE I: Lower and Upper Membership Functions for the IT2 Polynomial Fuzzy Model of the Inverted Pendulum.

Lower and upper membership functions	
$\underline{\mu}_{\tilde{M}_1^1}(f_1(\mathbf{x}(t))) = \underline{\mu}_{\tilde{M}_1^2}(f_1(\mathbf{x}(t))) = \frac{f_{1_{\max}} - f_1(\mathbf{x}(t))}{f_{1_{\max}} - f_{1_{\min}}}$; $\overline{\mu}_{\tilde{M}_1^3}(f_1(\mathbf{x}(t))) = \overline{\mu}_{\tilde{M}_1^4}(f_1(\mathbf{x}(t))) = \frac{f_1(\mathbf{x}(t)) - f_{1_{\min}}}{f_{1_{\max}} - f_{1_{\min}}}$; with $x_2(t) = 0, m_p = m_{p_{\max}} = 1$kg and $M_c = M_{c_{\min}} = 18$kg	$\underline{\mu}_{\tilde{M}_2^1}(f_2(\mathbf{x}(t))) = \underline{\mu}_{\tilde{M}_2^3}(f_2(\mathbf{x}(t))) = \frac{f_{2_{\max}} - f_2(\mathbf{x}(t))}{f_{2_{\max}} - f_{2_{\min}}}$; $\overline{\mu}_{\tilde{M}_2^2}(f_2(\mathbf{x}(t))) = \overline{\mu}_{\tilde{M}_2^4}(f_2(\mathbf{x}(t))) = \frac{f_2(\mathbf{x}(t)) - f_{2_{\min}}}{f_{2_{\max}} - f_{2_{\min}}}$ with $m_p = m_{p_{\max}} = 1$kg and $M_c = M_{c_{\max}} = 20$kg
$\overline{\mu}_{\tilde{M}_1^1}(f_1(\mathbf{x}(t))) = \overline{\mu}_{\tilde{M}_1^2}(f_1(\mathbf{x}(t))) = \frac{f_{1_{\max}} - f_1(\mathbf{x}(t))}{f_{1_{\max}} - f_{1_{\min}}}$; $\underline{\mu}_{\tilde{M}_1^3}(f_1(\mathbf{x}(t))) = \underline{\mu}_{\tilde{M}_1^4}(f_1(\mathbf{x}(t))) = \frac{f_1(\mathbf{x}(t)) - f_{1_{\min}}}{f_{1_{\max}} - f_{1_{\min}}}$; with $x_2(t) = x_{2_{\max}}, m_p = m_{p_{\max}} = 1$kg and $M_c = M_{c_{\min}} = 18$kg	$\overline{\mu}_{\tilde{M}_2^1}(f_2(\mathbf{x}(t))) = \overline{\mu}_{\tilde{M}_2^3}(f_2(\mathbf{x}(t))) = \frac{f_{2_{\max}} - f_2(\mathbf{x}(t))}{f_{2_{\max}} - f_{2_{\min}}}$ $\underline{\mu}_{\tilde{M}_2^2}(f_2(\mathbf{x}(t))) = \underline{\mu}_{\tilde{M}_2^4}(f_2(\mathbf{x}(t))) = \frac{f_2(\mathbf{x}(t)) - f_{2_{\min}}}{f_{2_{\max}} - f_{2_{\min}}}$; with $m_p = m_{p_{\min}} = 0.5$kg and $M_c = M_{c_{\min}} = 18$kg

$\mathbf{y}(t) = \mathbf{C}\mathbf{x}(t)$ where $\hat{\mathbf{x}}(t) = \mathbf{x}(t) = [x_1(t) \quad x_2(t)]^T = [\theta(t) \quad \dot{\theta}(t)]^T$, $x_1(t) \in [\frac{-5\pi}{12} \quad \frac{5\pi}{12}]$, $x_2(t) \in [-4 \quad 4]$, $\mathbf{A}_1(\mathbf{x}(t)) = \mathbf{A}_2(\mathbf{x}(t)) = \begin{bmatrix} 0 & 1 \\ f_{1_{\min}}(\mathbf{x}(t)) & 0 \end{bmatrix}$, $\mathbf{A}_3(\mathbf{x}(t)) = \mathbf{A}_4(\mathbf{x}(t)) = \begin{bmatrix} 0 & 1 \\ f_{1_{\max}}(\mathbf{x}(t)) & 0 \end{bmatrix}$, $\mathbf{B}_1(\mathbf{x}(t)) = \mathbf{B}_3(\mathbf{x}(t)) = \begin{bmatrix} 0 & f_{2_{\min}}(\mathbf{x}(t)) \end{bmatrix}^T$, $\mathbf{B}_2(\mathbf{x}(t)) = \mathbf{B}_4(\mathbf{x}(t)) = \begin{bmatrix} 0 & f_{2_{\max}}(\mathbf{x}(t)) \end{bmatrix}^T$ and $\mathbf{C} = \begin{bmatrix} 1 & 0 \\ 0 & 1 \end{bmatrix}$.

The lower and upper membership functions are defined in Table I, in which $f_1(\mathbf{x}(t))$ and $f_2(\mathbf{x}(t))$ are nonlinear terms defined as $f_1(\mathbf{x}(t)) = \frac{g - am_pSx_2(t)^2\cos(x_1(t))}{4S/3 - am_pS\cos^2(x_1(t))}\big(\frac{\sin(x_1(t))}{x_1(t)}\big)$ and $f_2(\mathbf{x}(t)) = \frac{-a\cos(x_1(t))}{4S/3 - am_pS\cos^2(x_1(t))}$. Through the Taylor series based approach in [42], the minimum and maximum values of $f_1(\mathbf{x}(t))$ and $f_2(\mathbf{x}(t))$ can be obtained in polynomial functions as $f_{1_{\min}}(\mathbf{x}(t)) = 0.12996x_1(t)^2 + 10.5323$, $f_{1_{\max}}(\mathbf{x}(t)) = 0.12996x_1(t)^2 + 15.3038$, $f_{2_{\min}}(\mathbf{x}(t)) = 0.0037x_1(t)^2 - 0.0828$ and $f_{2_{\max}}(\mathbf{x}(t)) = 0.0037x_1(t)^2 - 0.0249$. The lower and upper grades of membership are, respectively, $w_i^L(\mathbf{x}(t)) = \underline{\mu}_{\tilde{M}_1^i}(f_1(\mathbf{x}(t))) \times \underline{\mu}_{\tilde{M}_2^i}(f_2(\mathbf{x}(t))$ and $w_i^U(\mathbf{x}(t)) = \overline{\mu}_{\tilde{M}_1^i}(f_1(\mathbf{x}(t))) \times \overline{\mu}_{\tilde{M}_2^i}(f_2(\mathbf{x}(t)))$ for all i. The reference model is chosen as $\mathbf{A_r} = \begin{bmatrix} 0 & 1 \\ -4 & -4 \end{bmatrix}$, $\mathbf{B_r} = \begin{bmatrix} 0 & 1 \end{bmatrix}^T$ and $r(t) = 4\sin(0.3t)$.

Based on the IT2 polynomial fuzzy model, an IT2 SDOF polynomial fuzzy controller with 2 rules is employed to perform the tracking control by following (9) and (12).

It should be noted that in this case $y_1(t_\gamma) = x_1(t_\gamma)$ due to $\mathbf{C} = \begin{bmatrix} 1 & 0 \\ 0 & 1 \end{bmatrix}$ and $x_1(t_\gamma)$ will be adopted instead of $y_1(t_\gamma)$. The overall IT2 SDOF polynomial fuzzy controller is obtained as $\mathbf{u}(t) = \tilde{m}_1(x_1(t_\gamma))(\mathbf{F}_1(\mathbf{h}(t_\gamma))\mathbf{e_y}(t_\gamma) + \mathbf{G}_1(\mathbf{h}(t_\gamma))\mathbf{y_r}(t_\gamma)) + \tilde{m}_2(x_1(t_\gamma))(\mathbf{F}_2(\mathbf{h}(t_\gamma))\mathbf{e_y}(t_\gamma) + \mathbf{G}_2(\mathbf{h}(t_\gamma))\mathbf{y_r}(t_\gamma))$ where the upper and lower membership functions are chosen as : $\overline{m}_1(x_1(t_\gamma)) = \{0$ for $x_1(t_\gamma) < -\frac{5\pi}{12}$ or $x_1(t_\gamma) > \frac{5\pi}{12}$; $\frac{x_1(t_\gamma)+5\pi/12}{5\pi/12}$ for $-\frac{5\pi}{12} \leq x_1(t_\gamma) \leq 0$; $\frac{5\pi/12 - x_1(t_\gamma)}{5\pi/12}$ for $0 \leq x_1(t_\gamma) \leq \frac{5\pi}{12}\}$ and $\underline{m}_1(x_1(t_\gamma)) = \{0$ for $x_1(t_\gamma) < -\frac{5\pi}{12}$ or $x_1(t_\gamma) > \frac{5\pi}{12}$; $\frac{0.9(x_1(t_\gamma)+5\pi/12)}{5\pi/12}$ for $-\frac{5\pi}{12} \leq x_1(t_\gamma) \leq 0$; $\frac{0.9(5\pi/12 - x_1(t_\gamma))}{5\pi/12}$ for $0 \leq x_1(t_\gamma) \leq \frac{5\pi}{12}\}$, $\overline{m}_2(x_1(t_\gamma)) = 1 - \underline{m}_1(x_1(t_\gamma))$, $\underline{m}_2(x_1(t_\gamma)) = 1 - \overline{m}_1(x_1(t_\gamma))$, and $\tilde{m}_2(x_1(t_\gamma)) = 1 - \tilde{m}_1(x_1(t_\gamma))$; and $\underline{\kappa}_j(x_1(t_\gamma)) = \overline{\kappa}_j(x_1(t_\gamma)) = 0.5$, j = 1, 2.

The membership functions depend on $x_1(t)$ which is used to determine their bounds δ_{ijl}. Recalling that $x_1 \in [\frac{-5\pi}{12}, \frac{5\pi}{12}]$, it suggests that the lower and upper bounds of x_1 is $\underline{x}_1 = \frac{-5\pi}{12}$ and $\overline{x}_1 = \frac{5\pi}{12}$. The sampling period in this simulation is set as $h_s = 0.005$s. From the polynomial fuzzy model, we have $\dot{x_1}(t) = x_2(t) \in [-25 \quad 25]$ that it gives the largest variation of x_1 within the sampling period as $\int_t^{t+h_s} \dot{x_1}(\sigma)d\sigma \leq 25 \times h_s$, which is within the domain $[-0.125 \quad 0.125]$. As we did in the first example, this consideration will be verified by simulations. With this information, from Section III-B2, it can be obtained that $x_1(t_\gamma) \in [x_1(t) - 0.125, \quad x_1(t) + 0.125]$.

By dividing the operating domain $x_1(t)$ into 10 uniform sub-domains (i.e., L = 10), it can be obtained that $\underline{y}_{1_l} = \underline{x}_{1_l} = \frac{-6\pi}{12} + \frac{\pi}{12}l$ and $\overline{y}_{1_l} = \overline{x}_{1_l} = \frac{-5\pi}{12} + \frac{\pi}{12}l$, l = 1, 2, . . ., 10, which are the lower and upper bounds of the l-th operating sub-domain, respectively. It is chosen that $\mathbf{D} = \text{diag}\{1, 0\}$, which means only $y_1 = x_1$ of the output vector has been included as the state information to facilitate the stability analysis.

m_p is set as 1kg and M_c is set as 18kg, which are both within the bounds of uncertainty and not known by the IT2 SDOF polynomial fuzzy controller. To apply Theorem 2, we set $\varepsilon_1(\mathbf{y}) = \varepsilon_2(\tilde{\mathbf{x}}) = \varepsilon_3(\mathbf{x}, \mathbf{x_r}) = \varepsilon_4(\mathbf{x}, \mathbf{x_r}) = \varepsilon_5(\mathbf{x}, \mathbf{x_r}) = \varepsilon_6(\tilde{\mathbf{x}}) = 0.001$; $\mathbf{X}(\tilde{\mathbf{x}})$ is a polynomial of degree 0; $\tilde{\mathbf{x}}$ as a null vector; $\mathbf{M}_j(x_1(t_\gamma))$ and $\mathbf{N}_j(x_1(t_\gamma))$, j = 1, 2, are polynomials with monomials in x_1 of degree 0, $\mathbf{S}_l(x_1(t))$ is of degree 0. The feedback gains are obtained as $\mathbf{F}_1 = [3852.7564 \quad 2020.09610]$, $\mathbf{F}_2 = [2822.5654 \quad 1482.4192]$, $\mathbf{G}_1 = [-1.8970 \times 10^{-11} \quad -8.1558 \times 10^{-12}]$, $\mathbf{G}_2 = [-4.10707 \times 10^{-12} \quad 1.5208 \times 10^{-12}]$, $\mathbf{X} = \begin{bmatrix} 1.3248 & -2.4269 \\ -2.4269 & 5.6270 \end{bmatrix}$. The values of σ_1, σ_2 and σ_3 are obtained as 7.7796, 0.4194 and 0.5508, respectively.

The IT2 SDOF fuzzy controller is employed to control the nonlinear plant subject to the initial conditions $\mathbf{x}(0) = [\pi/12 \quad 0]^T$ and $\mathbf{x_r}(0) = [\pi/16 \quad 0]^T$. Simulation results of state response and control signal are shown in Fig. 2. It can be seen that the system states are able to follow those of the the reference model closely.

For comparison purposes, Theorem 1 is applied with $\varepsilon_1(\tilde{\mathbf{x}}) = \varepsilon_2(\tilde{\mathbf{x}}) = \varepsilon_3(\mathbf{x}, \mathbf{x_r}) = 0.001$ and the same degrees of feedback gains and $\tilde{\mathbf{x}}$ used above, no feasible solution is found which suggests that bringing the information of membership functions can help relax the stability analysis results. In addition, comparison has been made with the type-1 T-S system, where $m_1(x_1(t_\gamma)) = \{0$ for $x_1(t_\gamma) < -\frac{5\pi}{12}$ or $x_1(t_\gamma) > \frac{5\pi}{12}$; $\frac{x_1(t_\gamma)+5\pi/12}{5\pi/12}$ for $-\frac{5\pi}{12} \leq x_1(t_\gamma) \leq 0$; $\frac{5\pi/12 - x_1(t_\gamma)}{5\pi/12}$ for $0 \leq x_1(t_\gamma) \leq \frac{5\pi}{12}\}$, $m_2(x_1(t_\gamma)) = 1 - m_1(x_1(t_\gamma))$, $f_{1_{\min}}(\mathbf{x}(t)) = 10.5323$, $f_{1_{\max}}(\mathbf{x}(t)) = 15.5266$, $f_{2_{\min}}(\mathbf{x}(t)) = -0.0765$, $f_{2_{\max}}(\mathbf{x}(t)) = -0.0186$ and the rest parameters are the same. However, no feasible solution has been found, which verifies the effectiveness of proposed approach again.

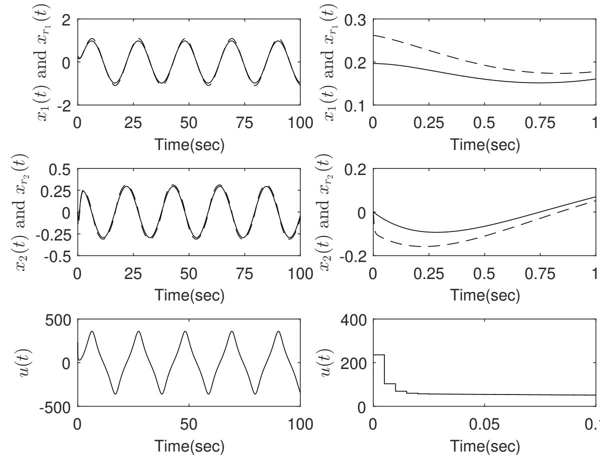

Fig. 2: Tracking control performance for $x_1(t)$ under 10 sub-domains, $\sigma_1 = 7.7796$, $\sigma_2 = 0.4194$ and $\sigma_3 = 0.5508$. Top left: responses of $x_1(t)$ (Dash line) and $x_{r_1}(t)$ (Solid line) from 0 to 100 seconds. Top right: responses of $x_1(t)$ (Dash line) and $x_{r_1}(t)$ (Solid line) from 0 to 1 second. Middle left: responses of $x_2(t)$ (Dash line) and $x_{r_2}(t)$ (Solid line) from 0 to 100 seconds. Middle right: responses of $x_2(t)$ (Dash line) and $x_{r_2}(t)$ (Solid line) from 0 to 1 second. Bottom left:$u(t)$ from 0 to 100 seconds. Bottom right: $u(t)$ from 0 to 1 second.

V. Conclusion

The SDOF tracking control problem for the IT2 PFMB control system has been investigated using the SOS-based analysis. An IT2 SDOF polynomial fuzzy controller has been employed to perform the tracking control, which is to drive the system states to follow those of a stable reference model characterized by H_∞ performance. Both MFI and MFD approaches are employed to conduct stability analysis. Under the MFD approach, the information of membership functions, system states and sampling process are utilized for the relaxation of stability analysis results. From the simulation examples, it can be shown that the MFD analysis approach helps relax the stability conditions. The comparison also shows the advantages of IT2 fuzzy systems over type-1 counterparts. In the future, the MFD approach can be extended to other applications like time-delay control systems, cost-guaranteed control system, noisy measurement and model reduction.

References

[1] K. Tanaka and H. O. Wang, *Fuzzy control systems design and analysis: a linear matrix inequality approach.* John Wiley & Sons, 2004.

[2] S. Blažič, I. Škrjanc, and D. Matko, "Globally stable direct fuzzy model reference adaptive control," *Fuzzy Sets Syst.*, vol. 139, no. 1, pp. 3–33, 2003.

[3] A. Sala and C. Ariño, "Asymptotically necessary and sufficient conditions for stability and performance in fuzzy control: Applications of Polya's theorem," *Fuzzy Sets Syst.*, vol. 158, no. 24, pp. 2671–2686, Jul. 2007.

[4] R.-E. Precup, M. L. Tomescu, S. Preitl, E. M. Petriu, J. Fodor, and C. Pozna, "Stability analysis and design of a class of MIMO fuzzy control systems," *Journal of Intelligent & Fuzzy Systems*, vol. 25, no. 1, pp. 145–155, 2013.

[5] S. Vrkalovic, T.-A. Teban, and I.-D. Borlea, "Stable takagi-sugeno fuzzy control designed by optimization," *Int. J. Artif. Intell*, vol. 15, no. 2, pp. 17–29, 2017.

[6] Y. Wei, J. Qiu, P. Shi, and M. Chadli, "Fixed-order piecewise-affine output feedback controller for fuzzy-affine-model-based nonlinear systems with time-varying delay," *IEEE Trans. Circuits Syst. I, Reg. Papers*, vol. 64, no. 4, pp. 945–958, 2017.

[7] Y. Wei, J. Qiu, P. Shi, and L. Wu, "A piecewise-markovian lyapunov approach to reliable output feedback control for fuzzy-affine systems with time-delays and actuator faults," *IEEE Trans. cybern.*, vol. 48, no. 9, pp. 2723–2735, 2018.

[8] C.-S. Tseng, B.-S. Chen, and H.-J. Uang, "Fuzzy tracking control design for nonlinear dynamic systems via ts fuzzy model," *IEEE Trans. Fuzzy Syst.*, vol. 9, no. 3, pp. 381–392, 2001.

[9] J.-C. Lo and M.-L. Lin, "Robust H_∞ nonlinear control via fuzzy static output feedback," *IEEE Trans. Circuits Syst. I, Fundam. Theory Appl.*, vol. 50, no. 11, pp. 1494–1502, 2003.

[10] S. K. Nguang and P. Shi, "Fuzzy output feedback control of nonlinear systems under sampled measurements," *Automatica*, vol. 39, no. 12, pp. 2169–2174, Dec. 2003.

[11] K. Y. Lian and J. J. Liou, "Output tracking control for fuzzy systems via output feedback design," *IEEE Trans. Fuzzy Syst.*, vol. 14, no. 5, pp. 628–639, Oct. 2006.

[12] B. Mansouri, N. Manamanni, K. Guelton, A. Kruszewski, and T. M. Guerra, "Output feedback LMI tracking control conditions with H_∞ criterion for uncertain and disturbed T-S models," *Inf. Sci.*, vol. 179, no. 4, pp. 446–457, Feb. 2009.

[13] H. K. Lam and L. D. Seneviratne, "Tracking control of sampled-data fuzzy-model-based control systems," *IET Control Theory Appl.*, vol. 3, no. 1, pp. 56–67, Jan. 2009.

[14] H. K. Lam, "Stabilization of nonlinear systems using sampled-data output-feedback fuzzy controller based on polynomial-fuzzy-model-based control approach," *IEEE Trans. Syst., Man and Cybern. B, Cybern.*, vol. 42, no. 1, pp. 258–267, 2012.

[15] H. K. Lam and H. Li, "Output-feedback tracking control for polynomial fuzzy-model-based control systems," *IEEE Trans. Ind. Electron.*, vol. 60, no. 12, pp. 5830–5840, 2013.

[16] K. Tanaka, H. Yoshida, H. Ohtake, and H. O. Wang, "A sum-of-squares approach to modeling and control of nonlinear dynamical systems with polynomial fuzzy systems," *IEEE Trans. Fuzzy Syst.*, vol. 17, no. 4, pp. 911–922, 2009.

[17] J. M. Mendel, "Type-2 fuzzy sets and systems: an overview," *IEEE Comput. Intell. Mag.*, vol. 2, no. 1, pp. 20–29, 2007.

[18] H. K. Lam and L. D. Seneviratne, "Stability analysis of interval type-2 fuzzy-model-based control systems," *IEEE Trans. Syst., Man and Cybern. B, Cybern.*, vol. 38, no. 3, pp. 617–628, 2008.

[19] H. K. Lam, H. Li, C. Deters, E. Secco, H. A. Wurdemann, and K. Althoefer, "Control design for interval type-2 fuzzy systems under imperfect premise matching," *IEEE Trans. Ind. Electron.*, vol. 61, no. 2, pp. 956–968, 2014.

[20] H. Li, X. Sun, P. Shi, and H. K. Lam, "Control design of interval type-2 fuzzy systems with actuator fault: Sampled-data control approach," *Inf. Sci.*, vol. 32, pp. 1–13, May 2015.

[21] B. Xiao, H. K. Lam, and H. Li, "Stabilization of interval type-2 polynomial-fuzzy-model-based control systems," *IEEE Trans. Fuzzy Syst.*, vol. 25, no. 1, pp. 205–217, Feb. 2017.

[22] R. Sakthivel, S. Karthick, B. Kaviarasan, and F. Alzahrani, "Dissipativity-based non-fragile sampled-data control design of interval type-2 fuzzy systems subject to random delays," *ISA trans.*, vol. 83, pp. 154–164, 2018.

[23] T. Zhao, J. Liu, and S. Dian, "Finite-time control for interval type-2 fuzzy time-delay systems with norm-bounded uncertainties and limited communication capacity," *Inf. Sci.*, 2019.

[24] X. Sun, H. Zhang, Q. Shan, and Y. Wang, "H_∞ control of interval type-2 fuzzy logic system with time-delay partition method," *Neurocomputing*, vol. 275, pp. 200–207, 2018.

[25] M. A. Sanchez, O. Castillo, and J. R. Castro, "Generalized type-2 fuzzy systems for controlling a mobile robot and a performance comparison with interval type-2 and type-1 fuzzy systems," *Expert Syst. Appl.*, vol. 42, no. 14, pp. 5904–5914, 2015.

[26] L. Cervantes and O. Castillo, "Type-2 fuzzy logic aggregation of multiple fuzzy controllers for airplane flight control," *Inf. Sci.*, vol. 324, pp. 247–256, 2015.

[27] M. A. Sanchez, O. Castillo, and J. R. Castro, "Information granule formation via the concept of uncertainty-based information with interval type-2 fuzzy sets representation and Takagi-Sugeno-Kang consequents optimized with cuckoo search," *Appl. Soft Comput.*, vol. 27, pp. 602–609, 2015.

[28] O. Castillo, L. Amador-Angulo, J. R. Castro, and M. Garcia-Valdez, "A comparative study of type-1 fuzzy logic systems, interval type-2 fuzzy logic systems and generalized type-2 fuzzy logic systems in control problems," *Inf. Sci.*, vol. 354, pp. 257–274, 2016.

[29] O. Castillo, L. Cervantes, J. Soria, M. Sanchez, and J. R. Castro, "A generalized type-2 fuzzy granular approach with applications to aerospace," *Inf. Sci.*, vol. 354, pp. 165–177, 2016.

[30] L. Cervantes, O. Castillo, D. Hidalgo, and R. Martinez-Soto, "Fuzzy dynamic adaptation of gap generation and mutation in genetic optimization of type 2 fuzzy controllers," *Advances in Operations Research*, vol. 2018, 2018.

[31] E. Ontiveros-Robles, P. Melin, and O. Castillo, "Comparative analysis of noise robustness of type 2 fuzzy logic controllers," *Kybernetika*, vol. 54, no. 1, pp. 175–201, 2018.

[32] ——, "New methodology to approximate type-reduction based on a continuous root-finding Karnik Mendel algorithm," *Algorithms*, vol. 10, no. 3, p. 77, 2017.

[33] A. Sarabakha, C. Fu, E. Kayacan, and T. Kumbasar, "Type-2 fuzzy logic controllers made even simpler: From design to deployment for UAVs," *IEEE Trans. Ind. Electron.*, vol. 65, no. 6, pp. 5069–5077, 2018.

[34] H. K. Lam and F. H. Leung, "Design and stabilization of sampled-data neural-network-based control systems," *IEEE Trans. Syst., Man Cybern. B, Cybern.*, vol. 36, no. 5, pp. 995–1005, 2006.

[35] H. Katayama and A. Ichikawa, "H_∞ control for sampled-data nonlinear systems described by Takagi-Sugeno fuzzy systems," *Fuzzy Sets Syst.*, vol. 148, no. 3, pp. 431–452, 2004.

[36] X. Jiang, "On sampled-data fuzzy control design approach for T-S model-based fuzzy systems by using discretization approach," *Inf. Sci.*, vol. 296, pp. 307–314, Mar. 2015.

[37] H. J. Lee and D. Wan Kim, "Intelligent digital redesign revisited: Approximate discretization and stability limitation," *Fuzzy Sets Syst.*, vol. 159, no. 23, pp. 3221–3231, Dec. 2008.

[38] H. C. Sung, D. W. Kim, J. B. Park, and Y. H. Joo, "Robust digital control of fuzzy systems with parametric uncertainties: LMI-based digital redesign approach," *Fuzzy Sets Syst.*, vol. 161, no. 6, pp. 919–933, Mar. 2010.

[39] D. W. Kim and H. J. Lee, "Sampled-data observer-based output-feedback fuzzy stabilization of nonlinear systems: exact discrete-time design approach," *Fuzzy Sets Syst.*, vol. 201, pp. 20–39, Aug. 2012.

[40] H. K. Lam, "A review on stability analysis of continuous-time fuzzy-model-based control systems: From membership-function-independent to membership-function-dependent analysis," *Eng. Appl. Artif. Intell.*, vol. 67, pp. 390–408, 2018.

[41] K. Gu, "An integral inequality in the stability problem of time-delay systems," in *Proc. IEEE 39th Conf. Decision Control*, vol. 3. IEEE, 2000, pp. 2805–2810.

[42] A. Sala and C. Ario, "Polynomial fuzzy models for nonlinear control: a Taylor series approach," *IEEE Trans. Fuzzy Syst.*, vol. 17, no. 6, pp. 1284–1295, 2009.